Development 136, 2187-2197 (2009) doi:10.1242/dev.030544

Follistatin modulates a BMP autoregulatory loop to control the size and patterning of sensory domains in the developing tongue

Crestina L. Beites[1,*,†], Piper L. W. Hollenbeck[1,*], Joon Kim[1,*,‡], Robin Lovell-Badge[2], Arthur D. Lander[3] and Anne L. Calof[1,§]

The regenerative capacity of many placode-derived epithelial structures makes them of interest for understanding the molecular control of epithelial stem cells and their niches. Here, we investigate the interaction between the developing epithelium and its surrounding mesenchyme in one such system, the taste papillae and sensory taste buds of the mouse tongue. We identify follistatin (FST) as a mesenchymal factor that controls size, patterning and gustatory cell differentiation in developing taste papillae. FST limits expansion and differentiation of *Sox2*-expressing taste progenitor cells and negatively regulates the development of taste papillae in the lingual epithelium: in *Fst*$^{-/-}$ tongue, there is both ectopic development of *Sox2*-expressing taste progenitors and accelerated differentiation of gustatory cells. Loss of *Fst* leads to elevated activity and increased expression of epithelial *Bmp7*; the latter effect is consistent with BMP7 positive autoregulation, a phenomenon we demonstrate directly. We show that FST and BMP7 influence the activity and expression of other signaling systems that play important roles in the development of taste papillae and taste buds. In addition, using computational modeling, we show how aberrations in taste papillae patterning in *Fst*$^{-/-}$ mice could result from disruption of an FST-BMP7 regulatory circuit that normally suppresses noise in a process based on diffusion-driven instability. Because inactivation of *Bmp7* rescues many of the defects observed in *Fst*$^{-/-}$ tongue, we conclude that interactions between mesenchyme-derived FST and epithelial BMP7 play a central role in the morphogenesis, innervation and maintenance of taste buds and their stem/progenitor cells.

KEY WORDS: Mouse, Placode, Taste bud, Taste papilla, Mesenchyme, Stem cell, Progenitor cell, TGF-beta, SHH, Wnt, SOX2, FOXA2

INTRODUCTION

Many vertebrate epithelia display regularly spaced specializations, such as hair follicles, feather buds, mammary glands, tooth buds and taste papillae (Chuong et al., 2000), which develop from discrete epithelial swellings known as placodes (Baker and Bronner-Fraser, 2001; Mikkola and Millar, 2006; Schlosser, 2006; Streit, 2007). The patterning and differentiation of placodes appears to be the result of complex epithelial-mesenchymal interactions, often involving secreted factors such as Wnts, bone morphogenetic proteins (BMPs) and sonic hedgehog (SHH) (Jiang et al., 1999; Jung et al., 1998; Mikkola and Millar, 2006; Plikus et al., 2008). Many placode-derived tissues also regenerate, making them ideal for investigating epithelial stem cells and their niches (Blanpain et al., 2007; Kawauchi et al., 2004; Murray and Calof, 1999; Plikus et al., 2008; Watt et al., 2006). In mammals, placode-derived sensory systems provide some of the few examples of robust neuronal regeneration following injury (Murray and Calof, 1999); the tongue, for example, readily regenerates its sensory (gustatory) cells following damage or denervation (Beidler and Smallman, 1965; Cheal and Oakley, 1977).

[1]Department of Anatomy and Neurobiology and Center for Complex Biological Systems, University of California, Irvine, CA 92697, USA. [2]Division of Stem Cell Biology and Developmental Genetics, Medical Research Council, National Institute of Medical Research, The Ridgeway, Mill Hill, London NW7 1AA, UK. [3]Department of Developmental and Cell Biology and Center for Complex Biological Systems, University of California, Irvine, CA 92697, USA.

*These authors contributed equally to this work
†Present address: Department of Health Sciences, Collège Boréal, Sudbury, Ontario, P3A 6B1, Canada
‡Present address: Department of Neurosciences, University of California, San Diego, La Jolla, CA 92093, USA
§Author for correspondence (e-mail: alcalof@uci.edu)

Accepted 21 April 2009

The tongue contains two classes of epithelial appendages, called papillae, which develop from an initially uniform field of lingual epithelial cells: (1) taste papillae (circumvallate, fungiform, foliate), which contain taste buds, the gustatory sensory cells of which signal to the nerves of the geniculate ganglion (Barlow, 1999; Barlow, 2003; Krimm, 2007; Mistretta and Liu, 2006); and (2) filiform papillae, keratinized structures that are innervated by mechanosensory neurons of the trigeminal root ganglion (Oakley and Witt, 2004). Taste papillae are distributed on the dorsal surface of the tongue in a regularly spaced pattern, a characteristic shared with other types of epithelial appendages, such as hair follicles.

In recent years, much has been learned about the signals passed between epithelium and mesenchyme in hair follicle formation and regeneration (Alonso and Fuchs, 2006; Bitgood and McMahon, 1995; Chiang et al., 1999; Lyons et al., 1989; Plikus et al., 2008; Reddy et al., 2001; Suzuki et al., 2009; Wall et al., 1993), but in sensory systems such as the tongue, our understanding is much less complete. Within the lingual epithelium, Wnts, BMPs and SHH are all expressed and participate in taste papilla/bud development (Barlow, 1999; Barlow, 2003; Hall et al., 2003; Hall et al., 1999; Iwatsuki et al., 2007; Jung et al., 1999; Liu et al., 2007; Liu et al., 2004; Okubo et al., 2006; Zhou et al., 2006). However, within the lingual mesenchyme, few signals of potential importance have been identified (e.g. Alappat et al., 2005), despite evidence for their existence (Barlow, 2003; Mistretta and Liu, 2006).

Here we identify follistatin (FST), an antagonist of a subset of TGFβ superfamily molecules, as a mesenchyme-derived secreted polypeptide that is crucial for regulating the size, patterning and innervation of taste papillae and the gustatory cells within them. We show that loss of FST leads to changes in the regions where taste papillae form and affects the spatial patterning of taste papillae, the levels of Wnt activity and *Shh* expression, and the production and

differentiation of sensory cells. We present evidence that these alterations are the consequence of elevated BMP7 signaling, caused (1) directly, by loss of BMP7 antagonism (consequent to loss of FST) and (2) indirectly, via positive autoregulation of *Bmp7* expression. Finally, results of computational modeling experiments lead us to propose that one role of an FST-BMP7 regulatory circuit is to suppress spatial noise in the patterning of taste papillae.

MATERIALS AND METHODS

Animals

Fst$^{+/-}$ mice (Matzuk et al., 1995) and *Bmp7*$^{lacZ/+}$ mice (Godin et al., 1998) were maintained on a C57BL/6J background. *BAT-Gal* mice (Maretto et al., 2003) were maintained on a Swiss Webster background (Harlan). *Sox2*β-*geo* mice (Avilion et al., 2003), used to report *Sox2* expression, were maintained on a CD1 background (Charles River); the *Sox2*β-*geo* background does not affect the *Fst*$^{-/-}$ phenotype in the tongue (see Fig. S1 in the supplementary material). The day of vaginal plug appearance was designated embryonic day 0.5 (e0.5). All protocols for animal use were approved by the Institutional Animal Care and Use Committee of the University of California, Irvine.

In situ hybridization (ISH) and immunohistochemistry

Whole-mount and section ISH were performed according to published protocols (Kawauchi et al., 1999; Murray et al., 2003). Probes were generated from: 318 bp mouse *Fst* (Wu et al., 2003); 642 bp mouse *Shh* (Echelard et al., 1993); 748 bp mouse *Sox2* (1281-2029 bp of GenBank #X94127); 566 bp mouse *Foxa2* (Puelles et al., 2003); and 860 bp mouse *Bmp7* (Furuta et al., 1997). For β-galactosidase (β-gal) histochemistry (X-Gal staining), tissue was processed as described (Murray et al., 2003). After staining, tongues were dehydrated, cleared in 100% methyl salicylate for 30 minutes and photographed immediately. For detection of cells in S phase, timed-pregnant (e17.5) dams were given one intraperitoneal injection of 5-bromo-2′-deoxyuridine (BrdU; 50 μg/gm) 1 hour before sacrifice, and immunostaining for BrdU was performed as described (Murray et al., 2003), except that rat anti-BrdU was detected using a biotin-conjugated rabbit anti-rat secondary antibody and the Vectastain ABC Kit (Vector Laboratories), with HRP-avidin visualized using DAB histochemistry (Leinco, K107).

For immunostaining, sections were incubated overnight at 4°C with: mouse anti-β-gal (Developmental Studies Hybridoma Bank; 1:2); goat anti-SHH (R&D, AF464; 15 μg/ml); rabbit anti-keratins (Dako, Z0622; 1:400); rabbit anti-β-gal (5′-3′, 7-063110; 1:1000); rabbit anti-gustducin (Santa Cruz, sc-395; 1:100); rabbit anti-PGP9.5 (Abcam, 10404; 1:1000); or rabbit anti-phospho-Smad1,5,8 (Cell Signaling, 9511; 1:50). For immunofluorescence, sections were counterstained for 10 minutes in bisbenzimide (Hoechst 33258; 20 μg/ml) and visualized using appropriate secondary antibodies [Cy2-conjugated goat anti-rabbit (Jackson); TRITC goat anti-mouse (Zymed); Cy3-conjugated donkey anti-rabbit (Jackson); Cy2-conjugated donkey anti-goat (Jackson)]. For anti-PGP9.5 immunohistochemistry, biotinylated goat anti-rabbit antibody and the Vectastain ABC Kit were employed as described above.

Bromophenol Blue staining, histology and scanning electron microscopy (SEM)

Dissected tongues were stained with Bromophenol Blue according to published protocols (Jonker et al., 2004). For histological analysis, tongues were cryosectioned at 12 μm and stained with Hematoxylin and Eosin (Kawauchi et al., 2009). For SEM, tongues were processed as described (Zhou et al., 2006).

Tissue culture

Tongues from e12.0 embryos were dissected free of surrounding mandible in cold Earle's Balanced Salt Solution (Invitrogen) and cultured in Millicell-HA chambers (0.45 μm, Millipore) in an airtight chamber with 5% CO_2, 3% O_2, 92% air for 2 days. The medium (DMEM/F12) contained 0.5% heat-inactivated fetal bovine serum, 2% B27 additive and Pen/Strep (Invitrogen). Where indicated, recombinant human BMP7 (PeproTech; 1.5 μg/ml) was added.

Computational modeling

A rectangular domain $0<y<1$ and $0<x<1.5$ was divided into a 50×75 grid, and the value at each grid point assigned an initial value equal to the sum of the function $0.8[sin(15x)sin(15y)]^6$, which generates an evenly spaced array of 35 peaks, maximum value=0.8, and a noise value equal to 0.24 times a random number chosen from a log-normal distribution with a mean of 0.3 and a variance of 0.7. The grid was used as the initial conditions for solving the differential equation:

$$\frac{\partial u}{\partial t} = D\nabla^2 u + \frac{1}{v}\frac{u^2}{u^2+2} - ku,$$

where u represents the value at each grid point (a concentration of BMP7), d is a diffusion coefficient, v is a (uniform) concentration of FST, and k is a decay constant. This equation describes a system in which BMP7 exerts saturating auto-activation with half-maximal activity at a concentration of $\sqrt{2}$ and a Hill coefficient of 2, and FST exerts linear inhibition. Parameter values were d=0.0005, k=3 and v=0.0875 in the wild-type case, and v=0.07 in the *Fst*$^{-/-}$ mutant (this corresponds to a situation in which loss of FST results in a 25% increase in BMP7 specific activity). Boundary conditions were Neumann-type at all boundaries. The equation was solved using the Reaction Diffusion Lab Package (version 2.0) written by Selwyn Hollis in Mathematica (Wolfram Research), which is available at www.appliedsymbols.com.

RESULTS

Epithelial dysplasia and aberrant patterning of taste and mechanosensory papillae in *Fst*$^{-/-}$ mouse tongue

Fst mRNA is first observed in the tongue anlage at day 11.5 of gestation (e11.5) (Fig. 1A). By e12.5, *Fst* is expressed throughout the tongue mesenchyme subjacent to lingual epithelium, with patches of expression also evident in deeper developing muscle. At e13.5, a region of especially high *Fst* expression is evident in posterior tongue mesenchyme underlying the developing intermolar eminence (IE) (Fig. 1A, e13.5 inset) [the IE, which is located between the anterior fungiform papillae and the posterior circumvallate papilla (CV), contains only non-gustatory filiform papillae (Mistretta and Liu, 2006; Zhou et al., 2006)]. After e14.5, *Fst* expression declines, and is barely detectable at e16.5 except in deep lingual muscle. The timing of *Fst* expression in lingual mesenchyme corresponds to the period during which taste placodes form and the size and patterning of taste papillae are determined (Mistretta and Liu, 2006).

When tongues of mice null for *Fst* were examined, we noted no major difference in their overall size as compared with those of wild-type littermates (Fig. 1B,C; data not shown). However, a test to assess formation of the keratinized permeability barrier on the lingual surface (Bromophenol Blue dye exclusion; see Materials and methods) showed that the tongues of P0 *Fst*$^{-/-}$ pups had a dramatic increase in dye permeability (Fig. 1B). Notably, a region of the posterior tongue, anterior to the CV and normally completely impermeable to dye, was deeply stained by Bromophenol Blue in *Fst*$^{-/-}$ mice (Fig. 1B), indicating that the keratinized barrier of the epithelium is compromised. This finding prompted us to examine the epithelium at higher resolution.

Scanning electron micrographs (SEMs) performed at e17.5 revealed several interesting changes in *Fst*$^{-/-}$ tongue. First, whereas the posterior surface of the tongue normally exhibits a uniform cobblestone appearance owing to the presence of numerous filiform papillae, in *Fst*$^{-/-}$ tongue the posterior surface contained a prominent, smooth, raised region; this region was similar in shape to that which stained aberrantly with Bromophenol Blue (Fig. 1C, compare with 1B). This suggested a lack of filiform papillae in this region, an idea confirmed in histological sections (Fig. 1D, IE).

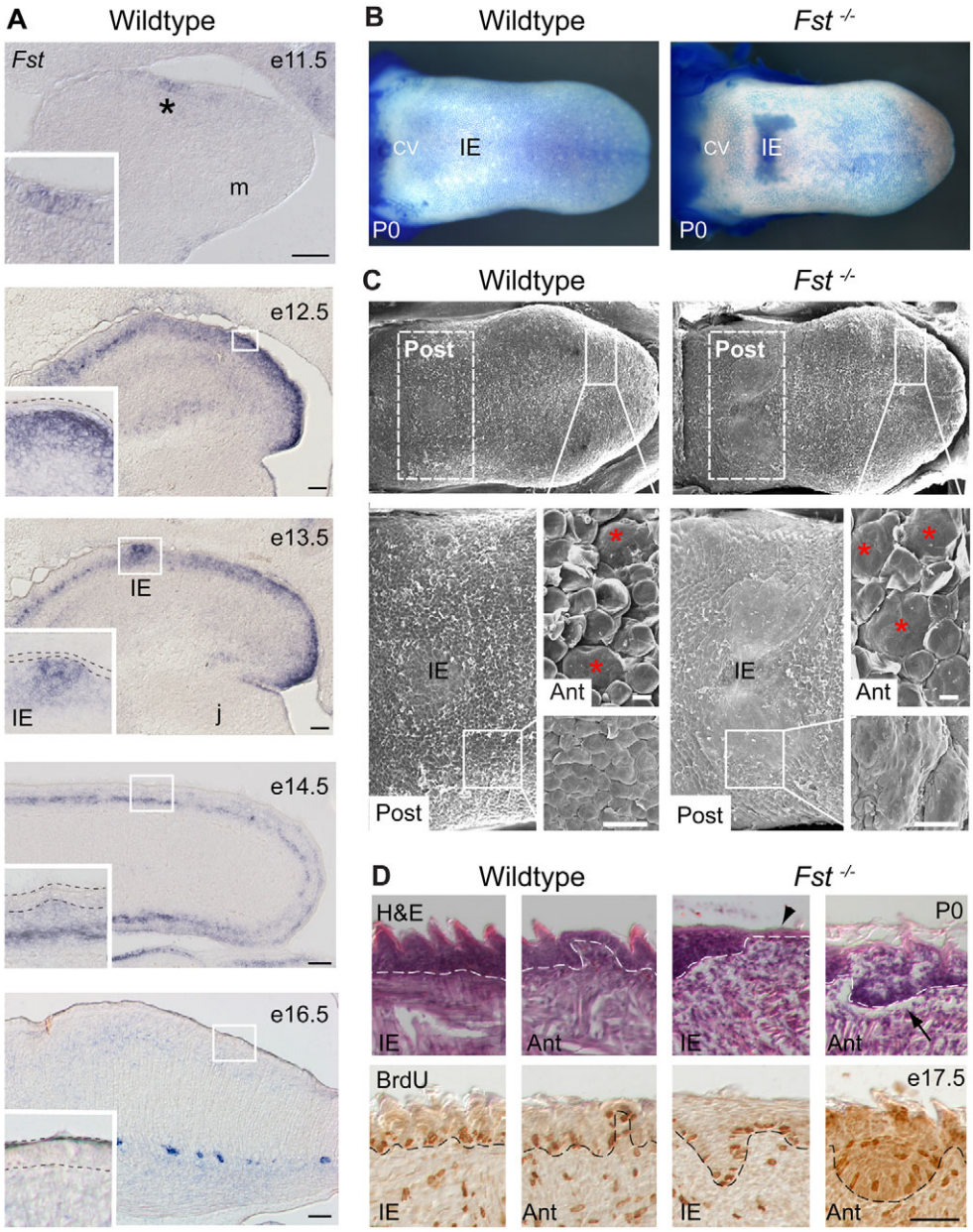

Fig. 1. *Fst* expression and *Fst*$^{-/-}$ phenotypes in the developing tongue. (**A**) In situ hybridization (ISH) analysis of *Fst* expression in wild-type mouse tongue. Asterisk, *Fst* expression in epithelium of tongue anlage; m, mandibular component of first branchial arch; IE, intermolar eminence; j, developing jaw. (**B**) P0 tongues stained with Bromophenol Blue. CV, circumvallate papilla. (**C**) SEM of e17.5 tongue from wild-type and *Fst*$^{-/-}$ mice. Red asterisks indicate fungiform papillae in the anterior tongue (Ant). Post, posterior tongue. (**D**) Hematoxylin and Eosin (H&E)-stained (P0) and BrdU-immunostained (e17.5) sections through IE and Ant regions of wild-type and *Fst*$^{-/-}$ tongue. Arrow and arrowhead in H&E-stained sections indicate regions of dysplastic epithelium (see text). Dashed lines in insets of A indicate apical and basal borders of lingual epithelium. Magnification is the same in all panels. Scale bars: 100 μm in A; 50 μm in D and in C, Post, highest magnification inset; 10 μm in C, Ant, highest magnification inset.

Thus, a distinctive phenotype of the *Fst*$^{-/-}$ tongue is a lack of filiform papillae on the epithelial surface of the posterior tongue. Also noted were changes in the size and spacing of fungiform papillae in the anterior region of the *Fst*$^{-/-}$ tongue. Although fungiform papillae were present in the mutant, they were irregular in size and often present in tight clusters, rather than showing their normal regular spacing (Fig. 1C, asterisks).

Histological staining revealed that the epithelium covering both the anterior and posterior tongue in *Fst*$^{-/-}$ mice was uneven in thickness, with multiple cell layers invaginating into underlying mesenchyme, as well as thinned areas of epithelium overlying domes of mesenchyme (Fig. 1D). These domes were reminiscent of fungiform papillae in shape, but tended not to protrude above the tongue surface (Fig. 1D, arrowhead). BrdU incorporation (to label cells in S phase) demonstrated that the epithelium of both wild-type and *Fst*$^{-/-}$ tongues contained proliferating cells, with no noticeable increase in the density of these cells, even in regions where the epithelium was thick and invaginated in the mutant (Fig. 1D).

Despite the morphological changes in filiform and fungiform papillae, we observed no major alterations in the morphology of either the CV or foliate papillae, both of which are present and contain identifiable taste buds in *Fst*$^{-/-}$ tongue (see Fig. S2A,B in the supplementary material). Lingual serous glands are also present, and of normal size and number, in *Fst*$^{-/-}$ tongue (see Fig. S2C in the supplementary material).

Expansion and ectopic development of *Sox2*-expressing domains in *Fst*$^{-/-}$ tongue

To determine the cellular composition of the dysplastic epithelium in *Fst*$^{-/-}$ tongue, we used *Sox2* as a marker for taste bud stem/progenitor cells (Okubo et al., 2006). For these experiments, we crossed a *Sox2* reporter allele [*Sox2*β-*geo* (Avilion et al., 2003)] onto the *Fst*$^{-/-}$ background to track *Sox2* expression using X-Gal histochemistry and anti-β-galactosidase immunostaining (see Materials and methods). In control tongue at e12.5, a low level of X-Gal staining (indicative of *Sox2* expression) was present in the

surface epithelium, with higher levels apparent in developing taste placodes (Fig. 2A). As development proceeded, X-Gal staining became confined to the taste buds proper (Fig. 2A, e17.5, inset), and was still evident in the taste buds of adult *Sox2*β-*geo* mice (data not shown).

At e14.5, the tongues of *Fst*$^{-/-}$; *Sox2*β-*geo* mice displayed noticeable disruptions in the pattern of X-Gal staining (Fig. 2E-G′). The X-Gal-stained domains in the apices of the developing fungiform papillae were visibly smaller in the mutant tongue than in the control (Fig. 2D′,G′, arrowheads). The epithelium in the anterior two-thirds of the mutant tongue was also thickened, and was lightly stained throughout (Fig. 2G′), foreshadowing the overt dysplasia and expanded staining evident a few days later. Interestingly, whereas the region containing the IE was free of *Sox2*-expressing taste papillae and devoid of X-Gal staining in control tongue at e14.5, in *Fst* nulls the same region displayed ectopic X-Gal staining: *Sox2*β-*geo* expression was evident in large clusters of epithelial cells (Fig. 2F) that invaginated into the underlying mesenchyme (Fig. 2F′, arrow). It is notable that the cells within these clusters expressed keratins, a known characteristic of lingual epithelium and taste buds (Luo et al., 2008; Mbiene and Roberts, 2003; Wong et al., 1994), despite their ectopic location, aberrant number and morphology (see Fig. S3 in the supplementary material).

At e17.5, expanded X-Gal staining and *Sox2*-expressing, invaginated epithelial cell clusters were prominent in the mutant tongue (Fig. 2K-M′). Disruption of the spacing of the fungiform papillae in the anterior region of the *Fst*$^{-/-}$ tongue was also more evident at e17.5 (compare Fig. 2J with 2M). In addition, large clusters of invaginating, X-Gal-stained cells were apparent in both the anterior and posterior regions of the mutant tongue at this stage (Fig. 2L′,M′, arrows); these were never observed in controls. Remarkably, the pattern of expanded X-Gal-stained cells in the posterior (IE) region of the mutant tongue corresponded closely to the raised, smoothened region of lingual epithelium seen by SEM and Bromophenol Blue staining (compare Fig. 2K with Fig. 1B,C).

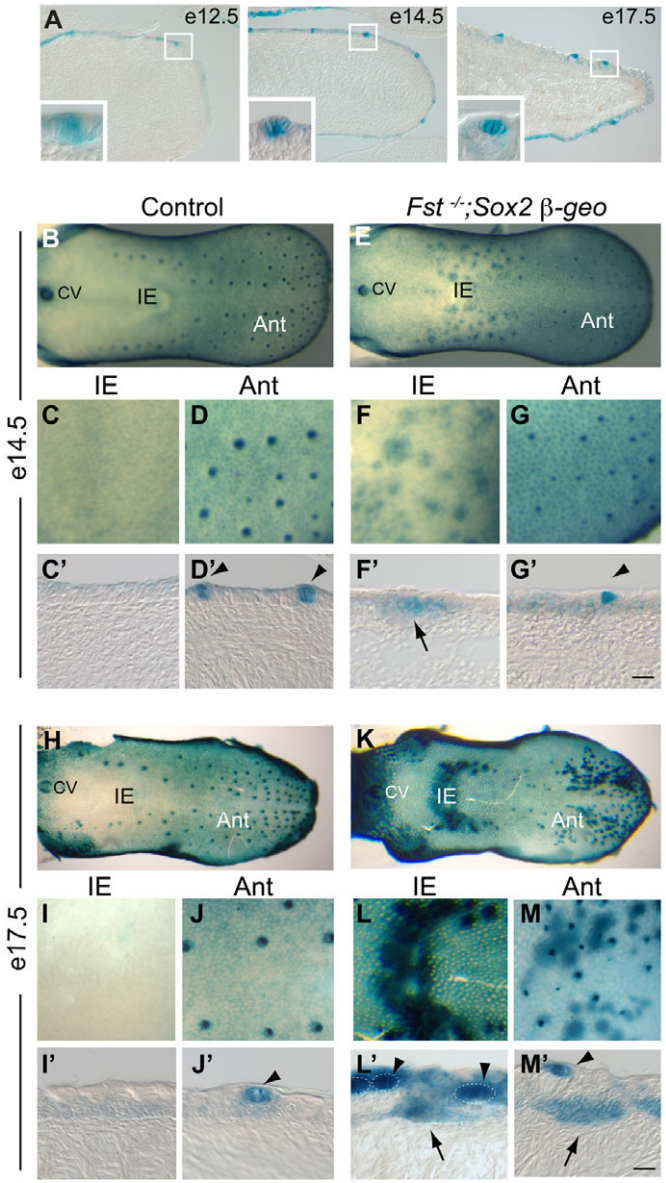

Fig. 2. Aberrant expression of *Sox2* in *Fst*$^{-/-}$ tongue. (**A**) Developmental expression of *Sox2*-β*geo* reporter detected by X-Gal staining in wild-type tongue. Insets are high magnifications of taste placodes/buds. (**B-M′**) *Sox2*-β*geo* expression detected by X-Gal staining of whole-mount (B-G,H-M) and sagittal sections (C′-G′,I′-M′) of tongues from e14.5 (B-G′) and e17.5 (H-M′) *Sox2*-β*geo* (control) and *Fst*$^{-/-}$; *Sox2*β-*geo* (mutant) mice. Arrowheads point to *Sox2*-β*geo* expression in developing fungiform papillae; at e14.5, X-Gal-stained taste bud cell clusters near the surface are significantly smaller in mutants [182.56±2.6 μm^2 (±s.d.)] than in controls [269.5±4.4 μm^2 (±s.d.)] (P=0.0017, Student's t-test). Arrows indicate areas of aberrant invaginated *Sox2*-β*geo*-expressing cells. CV, circumvallate papilla. Scale bars: 20 μm.

Shh expression and Wnt–β-catenin activity are reduced in *Fst* mutant tongue

Previous studies have identified an early requirement for SHH and Wnts in initiating and directing morphogenesis of fungiform papillae (Hall et al., 2003; Iwatsuki et al., 2007; Liu et al., 2004). Fig. 3 shows the effect of FST absence on these two signaling systems. In wild-type mice, *Shh* expression is detectable throughout the lingual epithelium at the time that taste placodes are initially forming (e12.5), in a diffuse pattern with elevated expression in placodal domains (similar to *Sox2*) (Fig. 2A; Fig. 3A). By e14.5, *Shh* expression becomes restricted to regions where fungiform taste papillae will develop in the anterior tongue, and by e17.5 only low-level expression in the taste buds, located in the apices of fungiform papillae, remains (Fig. 3A). In *Fst* mutants, by contrast, *Shh* expression in the anterior tongue was lower than normal at e12.5, markedly reduced at e14.5, and below the limits of detection by e17.5 (Fig. 3A). Interestingly, expression of *Shh* by the CV did not appear to be affected in *Fst*$^{-/-}$ tongue at any age examined, suggesting that development of this papilla is not controlled by FST.

To evaluate Wnt–β-catenin activity in *Fst*$^{-/-}$ tongue, the *BAT-Gal* reporter allele was bred onto the *Fst*$^{-/-}$ background. In BAT-Gal mice, *lacZ* is expressed under the control of β-catenin/TCF-response elements, so X-Gal staining reveals endogenous Wnt–β-catenin activity (Maretto et al., 2003). As shown in Fig. 3B, Wnt–β-catenin activity was decreased, compared with controls, in taste placodes in the anterior tongue of *Fst*$^{-/-}$ embryos at e12.5. Later in development, at e14.5 and e17.5, X-Gal-stained cell clusters were present in the anterior tongue of *Fst*$^{-/-}$; *BAT-Gal* mice, as well as in *BAT-Gal*$^{+/-}$ controls; however, the stained clusters in *Fst* nulls were noticeably reduced in size and overall X-Gal staining was reduced. X-Gal staining also revealed that the minimum distance between fungiform

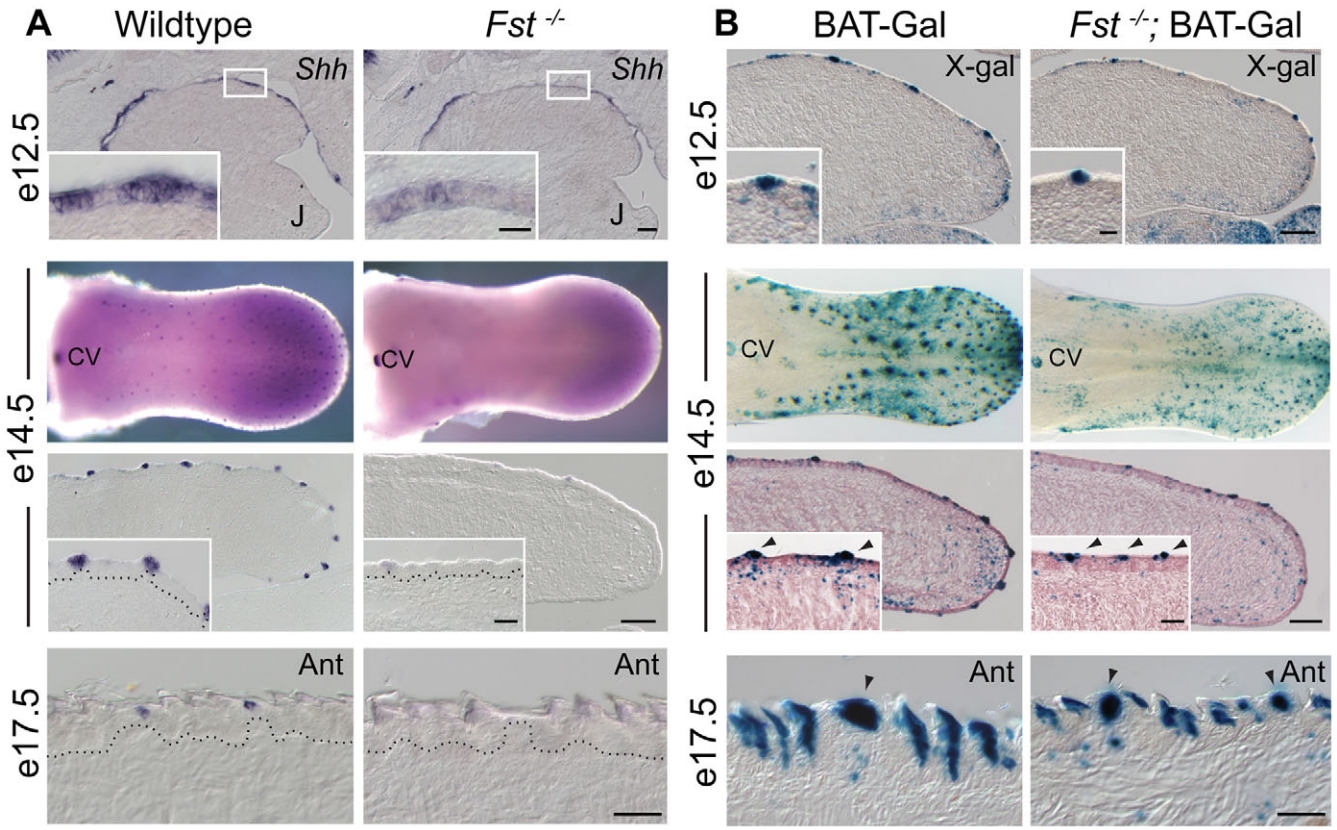

Fig. 3. *Shh* expression and Wnt–β-catenin activity are decreased in *Fst*$^{-/-}$ tongue. (**A**) ISH for *Shh* in tongues from wild-type and *Fst*$^{-/-}$ littermates at different developmental ages. Insets show higher magnifications of boxed regions (e12.5) and developing fungiform papillae (e14.5). J, jaw; CV, circumvallate papilla. (**B**) X-Gal staining of tongues of *BAT-Gal*$^{+/-}$ (control) and *Fst*$^{-/-}$*; BAT-Gal* mice at the same ages as in A. Arrowheads indicate developing fungiform papillae. Wnt–β-catenin activity is normally present in filiform papillae (Iwatsuki et al., 2007). Scale bars: e12.5, 100 μm (low power), 20 μm (insets); e14.5, 100 μm (low power), 50 μm (insets); e17.5, 50 μm.

papillae was altered (reduced) in *Fst*$^{-/-}$ tongue after e14.5 (Fig. 3B, arrowheads). This was quantified by counting the number of X-Gal-stained papillae per unit area in the anterior one-third of tongues of control (*BAT-Gal*$^{+/-}$) and *Fst*$^{-/-}$*; BAT-Gal* mice. The results (see Fig. S4 in the supplementary material) show a significant increase in the density of fungiform papillae in the tongue of *Fst* nulls as compared with control littermates [*Fst*$^{-/-}$*; BAT-Gal*, 47.9 (±3.8 s.e.m.) papillae per mm^2; *BAT-Gal*$^{+/-}$, 28.4 (±1.8 s.e.m.)].

Altogether, these findings are consistent with the observed reduction in the expression of *Sox2* and *Shh* in the developing fungiform papillae in the anterior region of *Fst*$^{-/-}$ tongue (Fig. 2M′; Fig. 3A). Moreover, they suggest that the defective formation and spacing of anterior taste papillae might be due to misregulation of Wnt and/or SHH signals in *Fst* nulls.

Loss of FST reveals gustatory competence of the epithelium of the intermolar eminence

The IE of the tongue is normally devoid of any taste papillae/buds. The observations that (1) the IE of *Fst*$^{-/-}$ tongue contains structures that morphologically resemble fungiform papillae (Fig. 1D), and (2) these ectopic ‘papillae’ express *Sox2* (Fig. 2), led us to speculate that the epithelium of the IE might take on some characteristics of true taste bud sensory cells (i.e. acquire gustatory competence) in the absence of FST. To test this, we examined the IE region of *Fst*$^{-/-}$ tongue for expression of taste bud/progenitor cell markers, for known components of the cytoplasmic taste-transduction pathway, and for innervation by cranial nerves. The results are shown in Fig. 4.

As demonstrated above (Figs 1 and 2), the IE region of *Fst*$^{-/-}$ tongue loses filiform papillae and takes on expression of *Sox2*, a marker for stem/progenitor cells of the fungiform papillae (Okubo et al., 2006). In sections through the IE of *Fst*$^{-/-}$ tongue processed for ISH, *Sox2* expression was present in clusters of invaginating epithelial cells that resembled ectopic, dysplastic taste papillae (Fig. 4A). The epithelium of the IE region in *Fst*$^{-/-}$ tongue also displayed discrete patches of both *Shh* expression and Wnt–β-catenin activity: these were never observed in the IE of wild-type controls (Fig. 4A).

Functional taste papillae are innervated by lingual nerves (Krimm, 2007; Ringstedt et al., 1999). To address whether the ectopic papillae in the IE of *Fst*$^{-/-}$ tongue acquire this characteristic, we used an antibody to the pan-neuronal marker PGP9.5 (UCHL1 – Mouse Genome Informatics) (Liu et al., 2007). As shown in Fig. 4B, mutant IE contained nerve fibers that extended into the cores of ectopic, SOX2-expressing papillae. We detected ingrowing PGP9.5-positive nerve fibers in 44% (173/394) of IE fields in *Fst* nulls, whereas innervation was never detected in the IE of wild-type tongue (0/143 fields). In addition to providing evidence for the acquisition of another functional characteristic by the ectopic taste papillae of *Fst*$^{-/-}$ IE, these findings provide evidence that it is the presence of taste papillae within the tongue that controls the ingrowth of nerves into the presumptive sensory field.

Transduction of chemical signals by the taste buds in fungiform papillae requires not only innervation, but also maturation of taste receptor cells within the taste buds. This process includes expression of gustducin (a component of the T1R family of G-protein-coupled

taste receptors; also known as GNAT3). We found that gustducin is expressed in the ectopic taste papillae that develop in the IE of *Fst*$^{-/-}$ tongue, whereas gustducin is never expressed in the IE of wild-type tongue (Fig. 4C). It is notable that gustducin was expressed only in small subsets of cells in the apical region of the much larger, SOX2-expressing domains of the ectopic taste papillae (Fig. 4C, arrowheads). Similarly, the ectopic expression of *Shh* and Wnt–β-catenin activity observed in the IE of *Fst*$^{-/-}$ tongue was also seen in the apical region of the epithelium (Fig. 4A). These observations raise the possibility that although SOX2 expression marks cells as competent to develop into functional taste bud cells (Okubo et al., 2006), and FST is crucial for normal expression of SOX2 (Fig. 2, above), other factors – such as Wnts and SHH – are required for full differentiation of SOX2-expressing progenitors into functional taste receptor cells (Iwatsuki et al., 2007; Liu et al., 2007; Liu et al., 2004; Okubo et al., 2008; Okubo et al., 2006).

We also noted that gustducin appears to be expressed prematurely in SOX2-expressing papillae in the anterior tongue of *Fst*$^{-/-}$ mice, being detectable as early as e17.5 (Fig. 4C, Ant; data not shown). Published reports indicate that gustducin expression normally does not occur until after birth in rodents (Wong et al., 1999; Zhang et al., 2007). This suggests that taste receptor cells in anterior fungiform papillae undergo accelerated differentiation in the absence of FST. Additionally, the observation that SOX2 and gustducin are co-expressed in individual cells of ectopic taste papillae (Fig. 4C, arrowheads) suggests a lineage relationship between SOX2-positive

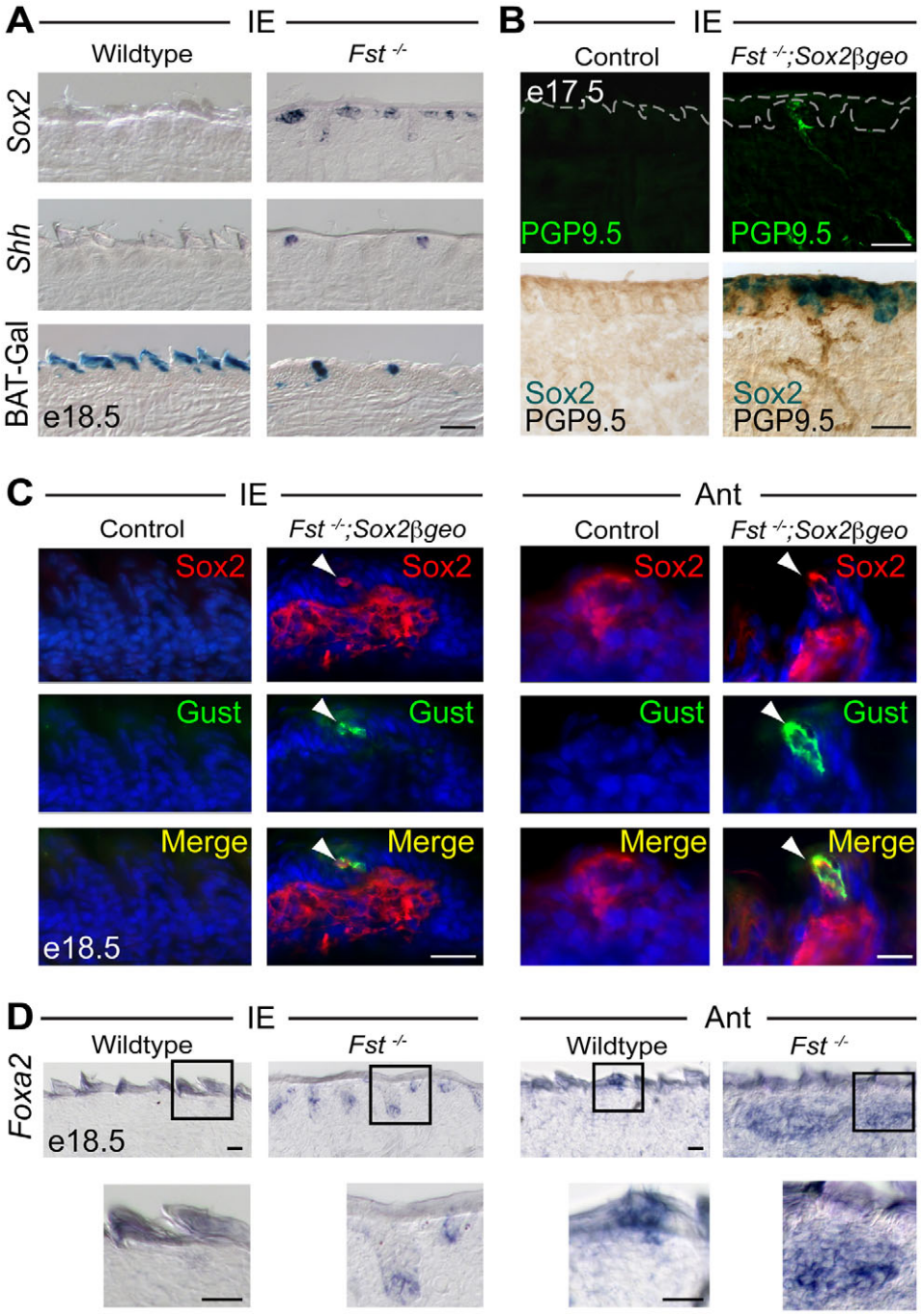

Fig. 4. Ectopic development and innervation of gustatory cell domains in *Fst*$^{-/-}$ tongue. (**A**) ISH for *Sox2* and *Shh*, and X-Gal staining for Wnt–β-catenin activity (BAT-Gal), in the IE of wild-type and *Fst*$^{-/-}$ mouse tongues at e18.5. (**B**) (Top) Immunofluorescence for PGP9.5 in sagittal sections of tongue to detect ingrowing nerve fibers in the IE of wild-type and *Fst*$^{-/-}$ tongues at e17.5. (Bottom) Combined X-Gal staining (to detect the *Sox2*-β*geo* reporter) and HRP immunohistochemistry (to detect PGP9.5-immunoreactive nerve fibers) in sagittal sections of tongue at the same age. (**C**) Immunofluorescence for β-galactosidase (to detect the *Sox2*-β*geo* reporter) and gustducin in sections through the IE and anterior (Ant) regions of control and *Fst*$^{-/-}$; *Sox2*-β*geo* tongues at e18.5. To ensure that comparable sections of IE were analyzed in control and mutant tongues, the CV was used as a landmark. (**D**) ISH for *Foxa2* in wild-type and *Fst*$^{-/-}$ tongues at e18.5. Insets show higher magnifications of boxed regions. Scale bars: 50 μm in A,B; 20 μm in D and in IE in C; 10 μm in Ant in C.

taste bud stem/progenitor cells and mature taste receptor cells that express gustducin, a finding in agreement with recent fate-mapping studies (Okubo et al., 2008).

Foxa2 encodes a transcription factor that is expressed both in developing lingual epithelium and mature taste buds (Besnard et al., 2004; Luo et al., 2008). We used ISH to determine whether the ectopic taste papillae that form in the IE and anterior regions of the tongue of $Fst^{-/-}$ mice acquire this additional marker of sensory (taste) epithelium. As shown in Fig. 4D, *Foxa2* is not expressed in the posterior/IE region of the tongue in wild-type mice at e18.5. However, *Foxa2* was expressed in the invaginated clusters of epithelial cells present in the IE of $Fst^{-/-}$ mice at this age, and its pattern of expression mimicked that of *Sox2* (Fig. 4A). In agreement with others (Luo et al., 2008), we found that *Foxa2* is expressed within definitive taste buds in the anterior tongue at e18.5 (Fig. 4D). *Foxa2* was also expressed within the ectopic epithelial cell clusters that invaginate into the underlying mesenchyme in *Fst* nulls, a further indication that the cells in these clusters possess characteristics of definitive taste bud cells.

In summary, the data indicate that in the absence of FST, epithelial cells of the IE region of the posterior tongue acquire many characteristics of taste papillae, including innervation by lingual nerves and expression of markers characteristic of taste bud progenitor cells and gustatory sensory cells. Since (1) the CV remains unchanged in $Fst^{-/-}$ tongue (Figs 1-3), and (2) the ectopic papillae that form in the posterior region of $Fst^{-/-}$ tongue resemble, both histologically and by expression of a number of molecular markers, those that form in the anterior tongue of *Fst* nulls (Fig. 4), these observations suggest that an important function of FST is to suppress the formation of ectopic fungiform taste papillae in the IE region.

Follistatin regulates BMP7 signaling and expression

FST binds to and inhibits several ligands of the activin subfamily, members of which signal via phosphorylation of cytoplasmic SMAD2 and SMAD3; FST also functions as an inhibitor of BMP7, which signals via phosphorylation of SMADs 1, 5 and 8 (Amthor et al., 2002; Khokha et al., 2005; Schneyer et al., 2003; Schneyer et al., 1994; Sidis et al., 2006). In agreement with others (Nie, 2005), we found that *Bmp7* expression is first detectable in lingual epithelium at e11.5; later, expression extends throughout the anterior epithelium and then becomes progressively restricted, in anterior tongue, to taste buds of the fungiform papillae, with some patches of low-level expression in mesenchyme and muscle (see Fig. S5 in the supplementary material). In posterior tongue and IE, *Bmp7* expression is normally detectable only in the lingual glands by the time of birth (see Fig. S2 in the supplementary material; Fig. 5B).

Since BMPs have been shown to inhibit taste papilla development in culture (Zhou et al., 2006), whereas loss of FST causes ectopic taste papilla formation, we postulated that changes in BMP signaling might underlie the alterations in taste papilla development observed in $Fst^{-/-}$ tongue. To test this, we used anti-phospho-SMAD1,5,8 immunostaining. As shown in Fig. 5, elevated and ectopic phospho-SMAD1,5,8 immunostaining was evident in localized patches of invaginating epithelial cells (ectopic taste papillae) in both the anterior (Fig. 5A) and posterior (Fig. 5B, IE) regions of *Fst* mutant tongue. We also observed ectopic expression of *Bmp7* in these same invaginating epithelial cell clusters (Fig. 5). Together, these data indicate that FST suppresses both *Bmp7* expression and BMP7 signaling during normal tongue development, and suggest that this serves two functions: (1) to control the size and patterning of developing taste papillae in the anterior tongue; and (2) to suppress the formation of ectopic taste papillae in the posterior (IE) tongue. A summary of the developmental phenotypes in the tongue that result from the absence of *Fst* expression is given in Table S1 in the supplementary material.

Fst antagonizes auto-activation of *Bmp7* expression

To directly test the effects of elevated BMP7 signaling on taste papilla development, we cultured tongues in recombinant BMP7 and looked for changes in Wnt–β-catenin and SHH activity (both are suppressed in the anterior tongue of $Fst^{-/-}$ mice) (Fig. 3). The data (see Fig. S6 in the supplementary material) demonstrate that increasing BMP7 levels causes a significant reduction both in Wnt–β-catenin activity and in the number and size of SHH-positive taste buds on the dorsum of the anterior tongue. These effects strongly resemble the phenotypes observed in vivo in $Fst^{-/-}$ tongue (Fig. 3), supporting the idea that a primary role of *Fst* in taste bud development is the suppression of BMP7 activity.

If this idea is correct, then loss of *Bmp7* should compensate for loss of *Fst*. As shown in Fig. 6, this is the case. In $Fst^{-/-}; Bmp7^{-/-}$ mice, two of the most severe phenotypes observed in $Fst^{-/-}$ tongue – loss of the surface permeability barrier of the IE resulting from an absence of filiform papillae (Fig. 6A), and loss of *Shh* expression in developing taste buds (Fig. 6B) – were rescued. This result provides strong evidence that the actions of *Fst* in the development of taste papillae/buds are mediated through antagonism of BMP7.

The observation that *Bmp7* expression is markedly elevated and appears at ectopic locations in $Fst^{-/-}$ tongue (Fig. 5) suggests that BMP7 might positively regulate its own expression. This idea is further supported by the observation that substantial rescue of $Fst^{-/-}$ phenotypes can be achieved by loss of a single allele of *Bmp7* (Fig. 6A,B), a result which suggests that high BMP7 signaling might be required to maintain *Bmp7* expression. To directly test for *Bmp7* autoregulation, we cultured e12.0 tongues dissected from $Bmp7^{lacZ/+}$ mice, which contain a *lacZ* reporter gene inserted into the first coding exon of *Bmp7*, in the presence or absence of BMP7. X-Gal staining was then used as an assay for *Bmp7* promoter activity. As shown in Fig. 6C, tongues cultured in the presence of BMP7 showed upregulation of *Bmp7* promoter activity in both anterior and posterior lingual epithelium. These results indicate that *Bmp7* stimulates it own expression, most likely at the transcriptional level.

Interestingly, despite the ability of *Bmp7* mutations to rescue the tongue phenotypes of *Fst* mutants, we have so far observed no lingual abnormalities in mice mutant for *Bmp7* alone. Such mice have normal expression of taste bud markers in both anterior and posterior tongue (see Fig. S7 in the supplementary material), and SEM analysis demonstrates that both fungiform taste papillae and IE are of normal morphology in the mutant tongues (Fig. 6D).

Regulatory interactions between FST and BMP7 create a circuit for suppressing spatial noise in papilla patterning

The regular spacing of taste papillae on the tongue is reminiscent of the regular spacing of other epithelial appendages, such as hair and feathers. In recent years, evidence has emerged that such patterning is controlled by the mechanism of diffusion-driven instability, in which a diffusible molecule activates both its own expression and that of a diffusible inhibitor that acts over a greater

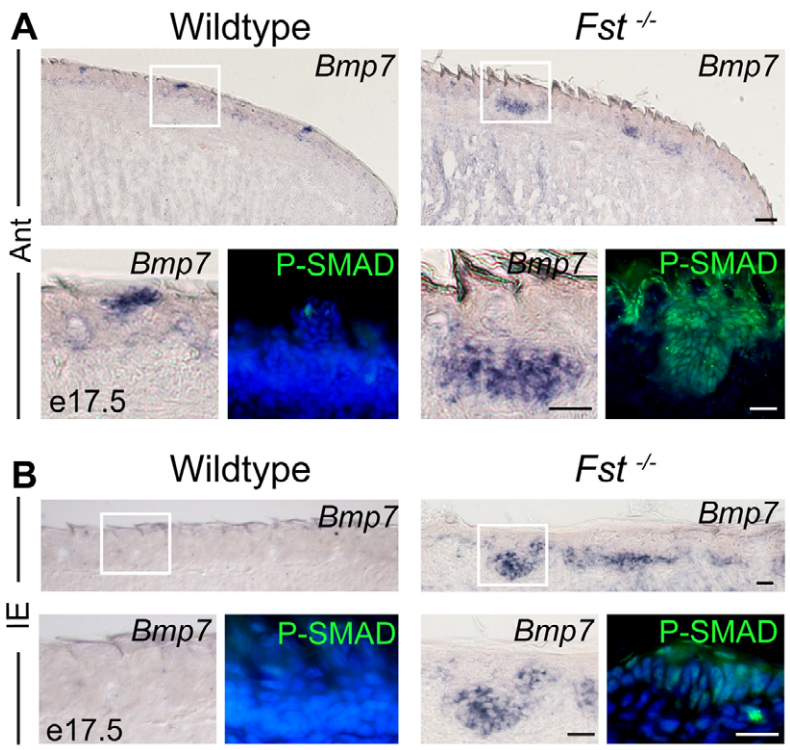

Fig. 5. Upregulation of *Bmp7* expression and signaling in *Fst*$^{-/-}$ tongue. (**A**,**B**) ISH for *Bmp7* (blue) and anti-phospho-SMAD1,5,8 (P-SMAD, green) immunostaining in sagittal sections of e17.5 wild-type and *Fst*$^{-/-}$ mouse tongues. *Bmp7* ISH insets show higher magnifications of boxed regions. P-SMAD immunofluorescence micrographs show comparable regions of anterior (A) or IE (B) tongue at higher magnification. Scale bars: 20 μm.

distance (Jiang et al., 1999; Jung et al., 1998; Maini et al., 2006; Sick et al., 2006). The ectopic formation and aberrant spacing of papillae in the *Fst*$^{-/-}$ tongue suggests that FST, through its role in suppressing BMP7 action, plays an important role in such a patterning process. However, as *Bmp7*$^{-/-}$ mice have well-patterned tongues (Fig. 6C; see Fig. S7 in the supplementary material), it seems unlikely that BMP7 and FST themselves form the activator/inhibitor pair that drives papilla patterning. In addition, although BMP7 does activate its own expression in the tongue (Fig. 6D), we find no evidence that it regulates expression of *Fst* (data not shown).

A more likely role for FST and BMP7 is in modulating a patterning system that is dependent on other factors, such as SHH and Wnts, both of which, along with SOX2, are crucial for taste papilla/bud development in the anterior tongue (Iwatsuki et al., 2007; Liu et al., 2007; Liu et al., 2004; Okubo et al., 2006). Our concept of how FST and BMP7 actions might regulate these processes to control development of fungiform taste papillae in the anterior tongue is illustrated in Fig. 7A. We conceive of an analogous process occurring in the IE, with the important difference that in the developing IE *Bmp7* expression is normally low or nil (Fig. 5B), whereas *Fst* expression is very high (Fig. 1A). This results in a lack of *Sox2* expression, so that the region normally produces only filiform (non-gustatory) papillae, rather than fungiform (gustatory) papillae (Fig. 1) (Okubo et al., 2006).

Using computational simulations, it is straightforward to show that any system with an auto-activating, diffusible signaling molecule (e.g. BMP7) and a ubiquitously expressed inhibitor (e.g. FST) will tend to act as a spatial noise filter. The findings from such a simulation for fungiform papilla development in anterior tongue are presented in Fig. 7B. They demonstrate how a weak and noisy pre-pattern of initial *Bmp7* expression converts itself, over time, into one that is strong and relatively noise-free ('wildtype'). Loss of *Fst* activity ('follistatin$^{-/-}$') under the same simulation conditions leads to domains of *Bmp7* expression that are abnormally large and less regularly spaced, much like those observed in the *Fst*$^{-/-}$ tongue (Fig. 5). Thus, a circuit comprising epithelial BMP7 and mesenchymal FST could play an important role in regulating the fidelity of patterning.

DISCUSSION

A role for epithelial-mesenchymal interactions in taste papilla morphogenesis has been proposed (e.g. Barlow, 2003; Mistretta and Liu, 2006), but relevant mesenchymal factors have not been identified previously. In this study, we show that FST, a secreted protein expressed in tongue mesenchyme, controls cell fate in the lingual epithelium and influences formation of the taste papillae that provide a niche for presumptive taste bud stem cells. FST regulates numerous biological processes through its ability to inhibit the activities of certain members of the TGFβ superfamily of secreted proteins (Balemans and Van Hul, 2002). In the tongue, we show that FST inhibits BMP7 activity, which in turn modulates signaling through the Wnt pathway, controls expression of *Shh*, *Sox2* and *Bmp7* itself, and influences spatial patterning. Support for the conclusion that FST acts primarily by regulating the function of BMP7 comes from the fact that loss of *Bmp7* can rescue the *Fst*$^{-/-}$ phenotype. However, we cannot exclude the possibility that FST also acts as an antagonist of other TGFβ family members to which it binds and that are present in the developing tongue (Nie, 2005; Sidis et al., 2006; Zhou et al., 2006).

Based on the available data, we propose that BMP7 plays at least two distinct, and partly antagonistic, roles in fungiform papilla development (Fig. 7A). The first role is in promoting the specification or stabilization of *Sox2*-positive progenitors that give rise to taste buds. *Sox2*, which is necessary and sufficient to drive lingual epithelial cells to differentiate into neural taste bud progenitors rather than keratinocytes [filiform papillae, in the case of the tongue (Okubo et al., 2006)], is initially expressed diffusely in lingual epithelium, but becomes progressively restricted to

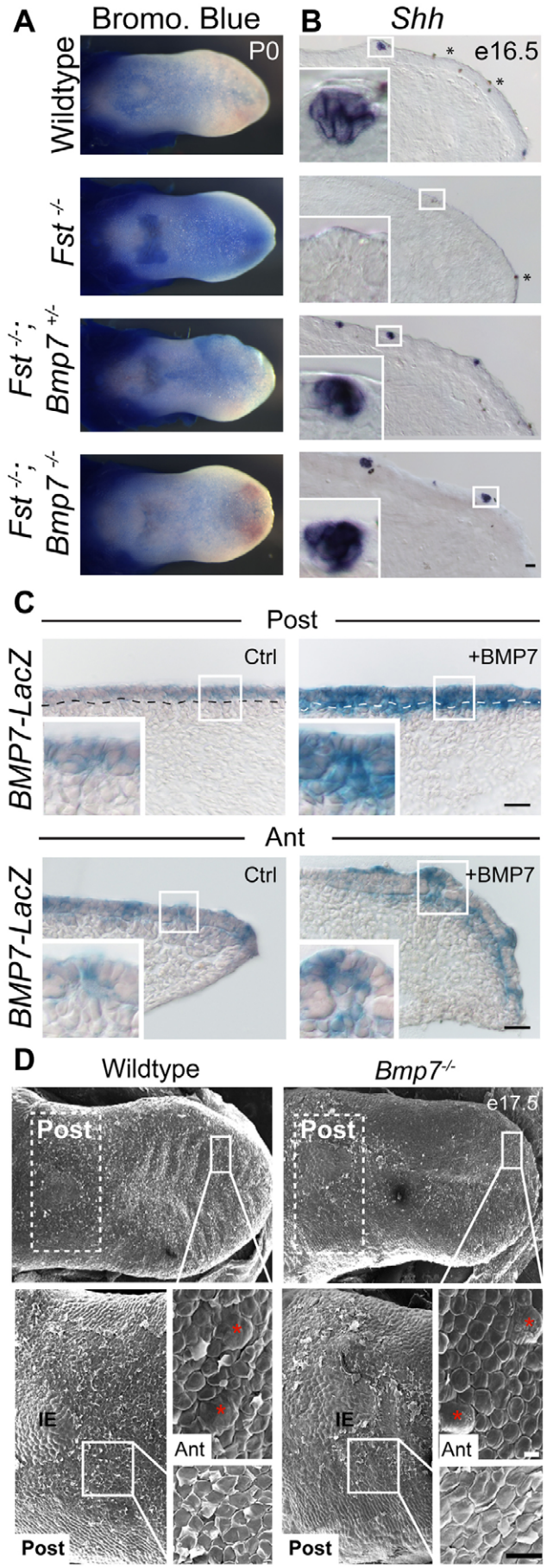

Fig. 6. Rescue of the *Fst*$^{-/-}$ phenotype by loss of *Bmp7* and demonstration of BMP7 auto-activation. (**A**) Tongues from P0 mice of indicated genotypes stained with Bromophenol Blue. (**B**) ISH analysis for *Shh* in e16.5 tongues of indicated genotypes. (**C**) Tongues from e12.0 *Bmp7*$^{lacZ/+}$ mice were cultured for 2 days in the absence (Ctrl) or presence (+BMP7) of BMP7, cryosectioned and stained with X-Gal. *n*=4 tongues per condition. (**D**) SEM of e17.5 wild-type and *Bmp7*$^{-/-}$ tongues. Fungiform papillae (red asterisks) in anterior (Ant) tongue are of normal size and spacing in *Bmp7*$^{-/-}$ mice. Filiform papillae in posterior tongue (Post) and IE are also normal. Asterisks denote artifacts from the ISH procedure. Scale bars: 20 μm in B,C; 10 μm in D, Ant high magnification, 50 μm in Post high magnification.

placodes of the developing taste papillae in the anterior tongue, where it is maintained at high levels in taste buds and taste papillae postnatally. Neighboring cells that differentiate into the keratinocytes of filiform papillae normally downregulate *Sox2* expression. Here we show that, in the absence of FST, cells that normally differentiate into keratinocytes maintain elevated levels of *Sox2* and, in at least some cases, appear to develop into taste buds expressing markers of taste transduction. Large numbers of ectopic *Sox2*-expressing cells also develop in the IE of *Fst* mutant tongue, and many of these cells are incorporated into fungiform papilla-like structures. The IE of *Fst*$^{-/-}$ tongue also loses its keratinized filiform papillae, suggesting that conversion of filiform papillae to gustatory, fungiform papillae is favored in the absence of FST. Furthermore, we found that ectopic taste papillae of both anterior and posterior *Fst*$^{-/-}$ tongue are innervated, suggesting that when the fate of the epithelium is altered, projecting nerve fibers can be redirected to new targets. These data advocate that neural competence is not an intrinsically determined aspect of tongue development, but rather one that is directed by interactions between the tongue epithelium and its underlying mesenchyme.

The second proposed role for BMP7 is in inhibiting a Wnt-SHH signaling circuit that maintains *Sox2*-positive cells within developing taste papillae that have already been specified. Within the fungiform papillae of *Fst* mutants, we observe coordinate downregulation of canonical Wnt signaling, *Shh* expression and *Sox2* expression (Fig. 2M′; Fig. 3A,B). Recent studies have indicated that canonical Wnt signaling promotes *Sox2* expression, which is required for taste papillae and taste bud development (Okubo et al., 2006) and induces expression of *Shh* (Liu et al., 2007). SHH in turn appears to act in a negative-feedback loop to antagonize Wnt activity (Iwatsuki et al., 2007). Therefore, the simplest explanation for the results we observe in the anterior tongue of *Fst*$^{-/-}$ mice is that reduction or loss of Wnt signaling, resulting from increased BMP7 activity, is the primary defect, with changes in *Shh* and *Sox2* expression being downstream consequences.

Because the effects of FST loss are rescued by a reduction in *Bmp7* dosage (Fig. 6A,B), and can be mimicked in vitro by the addition of BMP7 to wild-type tongues (see Fig. S6 in the supplementary material), we infer that BMP7 is a negative regulator of Wnt signaling in developing taste papillae. The fact that developing taste buds in the *Fst*$^{-/-}$ tongue are not only reduced in size, but also show the premature appearance of gustducin-positive cells (Fig. 4C), suggests that one mechanism of BMP7 action might be to promote stem/progenitor cell differentiation at the expense of self-replication. Inhibition of the Wnt pathway by BMP signaling has been reported in various tissues: for example, in hair follicles,

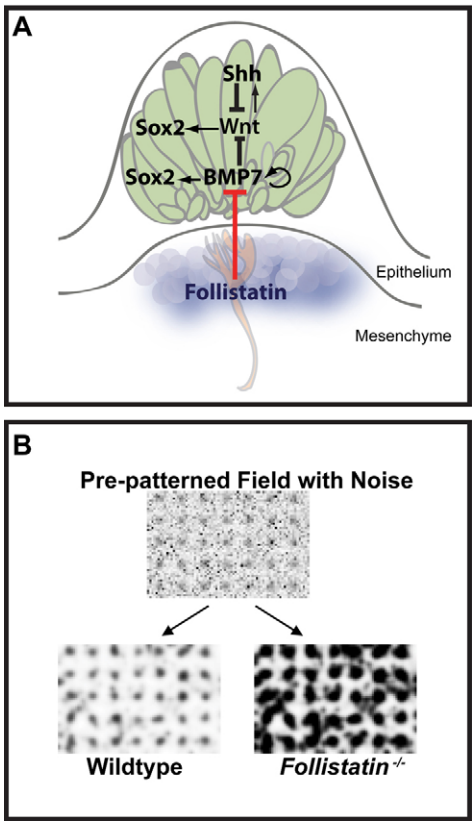

Fig. 7. FST and BMP7 form a regulatory circuit that regulates taste papilla formation and patterning in the developing mouse tongue. (**A**) Model illustrating how FST and BMP7 act to regulate SOX2 expression, Wnt–β-catenin signaling and SHH expression in developing fungiform papillae of the anterior tongue. (**B**) Representation of results from computational simulation showing how BMP7 and FST act to regulate the fidelity of taste papillae patterning in the developing anterior tongue. The complete simulation is given in Fig. S9 in the supplementary material. See main text for a detailed explanation.

BMPs suppress LEF1 activation via E-cadherin induction (Jamora et al., 2003); and in muscle, BMPs inhibit TCF expression (Bonafede et al., 2006).

The dual nature of the effect of BMP7 – promoting the allocation of progenitor cells to the taste bud fate while at the same time limiting the expansion of those cells – helps to explain why the *Fst*$^{-/-}$ phenotype is characterized both by too much *Sox2* expression in places where it should not be, and not enough *Sox2* expression in places where it should be. It also provides potential explanations for the regional differences in tongue patterning in wild-type and mutant animals. For example, in the IE, in which *Fst* expression levels are normally very high (Fig. 1A), inhibition of the role of BMP7 in specifying *Sox2*-expressing progenitors could explain why taste papillae are normally absent, yet appear in large numbers in the *Fst* mutant. In the anterior tongue, where *Fst* expression is normally not as high as in the IE (Fig. 1A), there is normally sufficient BMP7 signaling to allow taste papilla formation. Consequently, when BMP7 signaling is increased in the *Fst* mutant, a major phenotype is the reduced expression of taste bud markers, such as *Shh*, within those papillae (Fig. 3).

From the data presented here we may also infer that although FST/BMP7 might be necessary to induce the taste bud stem/progenitor cells of taste papillae, this is not sufficient to induce the morphological specializations of the papillae themselves. In *Fst*$^{-/-}$ tongue, many of the supernumerary *Sox2*-positive cells remain in clusters near the basal surface of the epithelium and do not become associated with morphological papillae. This suggests that taste papilla formation requires additional signals. Interestingly, our data indicate that such signals would need to be present in the IE, even though taste papillae normally never form there.

The notion that signals other than BMP7 dictate the locations of taste papillae also agrees with our suggestion that BMP7 does not primarily drive pattern formation, but rather improves its accuracy by suppressing noise (Fig. 7B; see Fig. S8 in the supplementary material). Patterns formed by diffusion-driven instability are intrinsically sensitive to spatial noise; indeed, the amplification of small, spatial non-uniformities is what can drive such systems to develop patterns spontaneously. In the tongue, the gradual conversion of uniform, low levels of Wnt signaling and *Shh* expression into regularly spaced puncta with high levels of Wnt activity and *Shh* expression, also suggests that pattern formation works through the amplification of subtle initial asymmetries. That the pattern becomes partially, but not completely, disorganized in the *Fst* mutant supports the view that BMP7 improves the ability of the patterning mechanism to distinguish such asymmetries from random variations in gene expression. Whether that patterning mechanism consists solely of the Wnt/SHH activator/inhibitor pair, or involves other molecules (such as DKK) (c.f. Sick et al., 2006), remains to be determined. Regardless, the results of this study clearly show that FST plays a major role in the epithelial-mesenchymal interactions that govern the morphogenesis of tongue epithelium.

We thank members of the Calof laboratory, especially Kimberly Kinga Gokoffski and Rosaysela Santos, for critical reading of the manuscript; and Dr Jian-Guo Zheng and the UCI Calit2 facility for assistance with the scanning electron microscopy. This work was supported by grants from the NIH to A.L.C. (DC03583, GM076516) and A.D.L. (GM076516), and by MRC funds to R.L.-B. Deposited in PMC for release after 6 months.

Supplementary material

Supplementary material for this article is available at http://dev.biologists.org/cgi/content/full/136/13/2187/DC1

References

Alappat, S. R., Zhang, Z., Suzuki, K., Zhang, X., Liu, H., Jiang, R., Yamada, G. and Chen, Y. (2005). The cellular and molecular etiology of the cleft secondary palate in Fgf10 mutant mice. *Dev. Biol.* **277**, 102-113.
Alonso, L. and Fuchs, E. (2006). The hair cycle. *J. Cell Sci.* **119**, 391-393.
Amthor, H., Christ, B., Rashid-Doubell, F., Kemp, C. F., Lang, E. and Patel, K. (2002). Follistatin regulates bone morphogenetic protein-7 (BMP-7) activity to stimulate embryonic muscle growth. *Dev. Biol.* **243**, 115-127.
Avilion, A. A., Nicolis, S. K., Pevny, L. H., Perez, L., Vivian, N. and Lovell-Badge, R. (2003). Multipotent cell lineages in early mouse development depend on SOX2 function. *Genes Dev.* **17**, 126-140.
Baker, C. V. and Bronner-Fraser, M. (2001). Vertebrate cranial placodes I. Embryonic induction. *Dev. Biol.* **232**, 1-61.
Balemans, W. and Van Hul, W. (2002). Extracellular regulation of BMP signaling in vertebrates: a cocktail of modulators. *Dev. Biol.* **250**, 231-250.
Barlow, L. A. (1999). A taste for development. *Neuron* **22**, 209-212.
Barlow, L. A. (2003). Toward a unified model of vertebrate taste bud development. *J. Comp. Neurol.* **457**, 107-110.
Beidler, L. M. and Smallman, R. L. (1965). Renewal of cells within taste buds. *J. Cell Biol.* **27**, 263-272.
Besnard, V., Wert, S. E., Hull, W. M. and Whitsett, J. A. (2004). Immunohistochemical localization of Foxa1 and Foxa2 in mouse embryos and adult tissues. *Gene Expr. Patterns* **5**, 193-208.
Bitgood, M. J. and McMahon, A. P. (1995). Hedgehog and Bmp genes are coexpressed at many diverse sites of cell-cell interaction in the mouse embryo. *Dev. Biol.* **172**, 126-138.
Blanpain, C., Horsley, V. and Fuchs, E. (2007). Epithelial stem cells: turning over new leaves. *Cell* **128**, 445-458.
Bonafede, A., Kohler, T., Rodriguez-Niedenfuhr, M. and Brand-Saberi, B. (2006). BMPs restrict the position of premuscle masses in the limb buds by influencing Tcf4 expression. *Dev. Biol.* **299**, 330-344.

Cheal, M. and Oakley, B. (1977). Regeneration of fungiform taste buds: temporal and spatial characteristics. *J. Comp. Neurol.* **172**, 609-626.
Chiang, C., Swan, R. Z., Grachtchouk, M., Bolinger, M., Litingtung, Y., Robertson, E. K., Cooper, M. K., Gaffield, W., Westphal, H., Beachy, P. A. et al. (1999). Essential role for Sonic hedgehog during hair follicle morphogenesis. *Dev. Biol.* **205**, 1-9.
Chuong, C. M., Patel, N., Lin, J., Jung, H. S. and Widelitz, R. B. (2000). Sonic hedgehog signaling pathway in vertebrate epithelial appendage morphogenesis: perspectives in development and evolution. *Cell Mol. Life Sci.* **57**, 1672-1681.
Echelard, Y., Epstein, D. J., St-Jacques, B., Shen, L., Mohler, J., McMahon, J. A. and McMahon, A. P. (1993). Sonic hedgehog, a member of a family of putative signaling molecules, is implicated in the regulation of CNS polarity. *Cell* **75**, 1417-1430.
Furuta, Y., Piston, D. W. and Hogan, B. L. (1997). Bone morphogenetic proteins (BMPs) as regulators of dorsal forebrain development. *Development* **124**, 2203-2212.
Godin, R. E., Takaesu, N. T., Robertson, E. J. and Dudley, A. T. (1998). Regulation of BMP7 expression during kidney development. *Development* **125**, 3473-3482.
Hall, J. M., Hooper, J. E. and Finger, T. E. (1999). Expression of sonic hedgehog, patched, and Gli1 in developing taste papillae of the mouse. *J. Comp. Neurol.* **406**, 143-155.
Hall, J. M., Bell, M. L. and Finger, T. E. (2003). Disruption of sonic hedgehog signaling alters growth and patterning of lingual taste papillae. *Dev. Biol.* **255**, 263-277.
Iwatsuki, K., Liu, H. X., Gronder, A., Singer, M. A., Lane, T. F., Grosschedl, R., Mistretta, C. M. and Margolskee, R. F. (2007). Wnt signaling interacts with Shh to regulate taste papilla development. *Proc. Natl. Acad. Sci. USA* **104**, 2253-2258.
Jamora, C., DasGupta, R., Kocieniewski, P. and Fuchs, E. (2003). Links between signal transduction, transcription and adhesion in epithelial bud development. *Nature* **422**, 317-322.
Jiang, T. X., Jung, H. S., Widelitz, R. B. and Chuong, C. M. (1999). Self-organization of periodic patterns by dissociated feather mesenchymal cells and the regulation of size, number and spacing of primordia. *Development* **126**, 4997-5009.
Jonker, L., Kist, R., Aw, A., Wappler, I. and Peters, H. (2004). Pax9 is required for filiform papilla development and suppresses skin-specific differentiation of the mammalian tongue epithelium. *Mech. Dev.* **121**, 1313-1322.
Jung, H. S., Francis-West, P. H., Widelitz, R. B., Jiang, T. X., Ting-Berreth, S., Tickle, C., Wolpert, L. and Chuong, C. M. (1998). Local inhibitory action of BMPs and their relationships with activators in feather formation: implications for periodic patterning. *Dev. Biol.* **196**, 11-23.
Jung, H. S., Oropeza, V. and Thesleff, I. (1999). Shh, Bmp-2, Bmp-4 and Fgf-8 are associated with initiation and patterning of mouse tongue papillae. *Mech. Dev.* **81**, 179-182.
Kawauchi, S., Takahashi, S., Nakajima, O., Ogino, H., Morita, M., Nishizawa, M., Yasuda, K. and Yamamoto, M. (1999). Regulation of lens fiber cell differentiation by transcription factor c-Maf. *J. Biol. Chem.* **274**, 19254-19260.
Kawauchi, S., Beites, C. L., Crocker, C. E., Wu, H. H., Bonnin, A., Murray, R. and Calof, A. L. (2004). Molecular signals regulating proliferation of stem and progenitor cells in mouse olfactory epithelium. *Dev. Neurosci.* **26**, 166-180.
Kawauchi, S., Kim, J., Santos, R., Wu, H.-H., Lander, A. D. and Calof, A. L. (2009). Foxg1 promotes olfactory neurogenesis by antagonizing Gdf11. *Development* **136**, 1453-1464.
Khokha, M. K., Yeh, J., Grammer, T. C. and Harland, R. M. (2005). Depletion of three BMP antagonists from Spemann's organizer leads to a catastrophic loss of dorsal structures. *Dev. Cell* **8**, 401-411.
Krimm, R. F. (2007). Factors that regulate embryonic gustatory development. *BMC Neurosci.* **8 Suppl. 3**, S4.
Liu, F., Thirumangalathu, S., Gallant, N. M., Yang, S. H., Stoick-Cooper, C. L., Reddy, S. T., Andl, T., Taketo, M. M., Dlugosz, A. A., Moon, R. T. et al. (2007). Wnt-beta-catenin signaling initiates taste papilla development. *Nat. Genet.* **39**, 106-112.
Liu, H. X., Maccallum, D. K., Edwards, C., Gaffield, W. and Mistretta, C. M. (2004). Sonic hedgehog exerts distinct, stage-specific effects on tongue and taste papilla development. *Dev. Biol.* **276**, 280-300.
Luo, X., Okubo, T., Randell, S. and Hogan, B. L. (2008). Culture of endodermal stem/progenitor cells of the mouse tongue. *In Vitro Cell. Dev. Biol. Anim.* **45**, 44-54.
Lyons, K. M., Pelton, R. W. and Hogan, B. L. (1989). Patterns of expression of murine Vgr-1 and BMP-2a RNA suggest that transforming growth factor-beta-like genes coordinately regulate aspects of embryonic development. *Genes Dev.* **3**, 1657-1668.
Maini, P. K., Baker, R. E. and Chuong, C. M. (2006). Developmental biology: the Turing model comes of molecular age. *Science* **314**, 1397-1398.
Maretto, S., Cordenonsi, M., Dupont, S., Braghetta, P., Broccoli, V., Hassan, A. B., Volpin, D., Bressan, G. M. and Piccolo, S. (2003). Mapping Wnt/beta-catenin signaling during mouse development and in colorectal tumors. *Proc. Natl. Acad. Sci. USA* **100**, 3299-3304.
Matzuk, M. M., Lu, N., Vogel, H., Sellheyer, K., Roop, D. R. and Bradley, A. (1995). Multiple defects and perinatal death in mice deficient in follistatin. *Nature* **374**, 360-363.
Mbiene, J. P. and Roberts, J. D. (2003). Distribution of keratin 8-containing cell clusters in mouse embryonic tongue: evidence for a prepattern for taste bud development. *J. Comp. Neurol.* **457**, 111-122.
Mikkola, M. L. and Millar, S. E. (2006). The mammary bud as a skin appendage: unique and shared aspects of development. *J. Mammary Gland Biol. Neoplasia* **11**, 187-203.
Mistretta, C. M. and Liu, H. X. (2006). Development of fungiform papillae: patterned lingual gustatory organs. *Arch. Histol. Cytol.* **69**, 199-208.
Murray, R. C. and Calof, A. L. (1999). Neuronal regeneration: lessons from the olfactory system. *Semin. Cell Dev. Biol.* **10**, 421-431.
Murray, R. C., Navi, D., Fesenko, J., Lander, A. D. and Calof, A. L. (2003). Widespread defects in the primary olfactory pathway caused by loss of Mash1 function. *J. Neurosci.* **23**, 1769-1780.
Nie, X. (2005). Apoptosis, proliferation and gene expression patterns in mouse developing tongue. *Anat. Embryol. (Berl.)* **210**, 125-132.
Oakley, B. and Witt, M. (2004). Building sensory receptors on the tongue. *J. Neurocytol.* **33**, 631-646.
Okubo, T., Pevny, L. H. and Hogan, B. L. (2006). Sox2 is required for development of taste bud sensory cells. *Genes Dev.* **20**, 2654-2659.
Okubo, T., Clark, C. and Hogan, B. L. (2008). Cell lineage mapping of taste bud cells and keratinocytes in the mouse tongue and soft palate. *Stem Cells* **27**, 442-450.
Plikus, M. V., Mayer, J. A., de la Cruz, D., Baker, R. E., Maini, P. K., Maxson, R. and Chuong, C. M. (2008). Cyclic dermal BMP signalling regulates stem cell activation during hair regeneration. *Nature* **451**, 340-344.
Puelles, E., Acampora, D., Lacroix, E., Signore, M., Annino, A., Tuorto, F., Filosa, S., Corte, G., Wurst, W., Ang, S. L. et al. (2003). Otx dose-dependent integrated control of antero-posterior and dorso-ventral patterning of midbrain. *Nat. Neurosci.* **6**, 453-460.
Reddy, S., Andl, T., Bagasra, A., Lu, M. M., Epstein, D. J., Morrisey, E. E. and Millar, S. E. (2001). Characterization of Wnt gene expression in developing and postnatal hair follicles and identification of Wnt5a as a target of Sonic hedgehog in hair follicle morphogenesis. *Mech. Dev.* **107**, 69-82.
Ringstedt, T., Ibanez, C. F. and Nosrat, C. A. (1999). Role of brain-derived neurotrophic factor in target invasion in the gustatory system. *J. Neurosci.* **19**, 3507-3518.
Schlosser, G. (2006). Induction and specification of cranial placodes. *Dev. Biol.* **294**, 303-351.
Schneyer, A., Schoen, A., Quigg, A. and Sidis, Y. (2003). Differential binding and neutralization of activins A and B by follistatin and follistatin like-3 (FSTL-3/FSRP/FLRG). *Endocrinology* **144**, 1671-1674.
Schneyer, A. L., Rzucidlo, D. A., Sluss, P. M. and Crowley, W. F., Jr (1994). Characterization of unique binding kinetics of follistatin and activin or inhibin in serum. *Endocrinology* **135**, 667-674.
Sick, S., Reinker, S., Timmer, J. and Schlake, T. (2006). WNT and DKK determine hair follicle spacing through a reaction-diffusion mechanism. *Science* **314**, 1447-1450.
Sidis, Y., Mukherjee, A., Keutmann, H., Delbaere, A., Sadatsuki, M. and Schneyer, A. (2006). Biological activity of follistatin isoforms and follistatin-like-3 is dependent on differential cell surface binding and specificity for activin, myostatin, and bone morphogenetic proteins. *Endocrinology* **147**, 3586-3597.
Streit, A. (2007). The preplacodal region: an ectodermal domain with multipotential progenitors that contribute to sense organs and cranial sensory ganglia. *Int. J. Dev. Biol.* **51**, 447-461.
Suzuki, K., Yamaguchi, Y., Villacorte, M., Mihara, K., Akiyama, M., Shimizu, H., Taketo, M. M., Nakagata, N., Tsukiyama, T., Yamaguchi, T. P. et al. (2009). Embryonic hair follicle fate change by augmented {beta}-catenin through Shh and Bmp signaling. *Development* **136**, 367-372.
Wall, N. A., Blessing, M., Wright, C. V. and Hogan, B. L. (1993). Biosynthesis and *in vivo* localization of the decapentaplegic-Vg-related protein, DVR-6 (bone morphogenetic protein-6). *J. Cell Biol.* **120**, 493-502.
Watt, F. M., Lo Celso, C. and Silva-Vargas, V. (2006). Epidermal stem cells: an update. *Curr. Opin. Genet. Dev.* **16**, 518-524.
Wong, G. T., Ruiz-Avila, L. and Margolskee, R. F. (1999). Directing gene expression to gustducin-positive taste receptor cells. *J. Neurosci.* **19**, 5802-5809.
Wong, L., Oakley, B., Lawton, A. and Shiba, Y. (1994). Keratin 19-like immunoreactivity in receptor cells of mammalian taste buds. *Chem. Senses* **19**, 251-264.
Wu, H. H., Ivkovic, S., Murray, R. C., Jaramillo, S., Lyons, K. M., Johnson, J. E. and Calof, A. L. (2003). Autoregulation of neurogenesis by GDF11. *Neuron* **37**, 197-207.
Zhang, G. H., Zhang, H. Y., Deng, S. P. and Qin, Y. M. (2007). Differentiation of alpha-gustducin in taste buds of the mouse soft palate and fungiform papillae. *Acta Histochem.* **109**, 486-490.
Zhou, Y., Liu, H. X. and Mistretta, C. M. (2006). Bone morphogenetic proteins and noggin: inhibiting and inducing fungiform taste papilla development. *Dev. Biol.* **297**, 198-213.

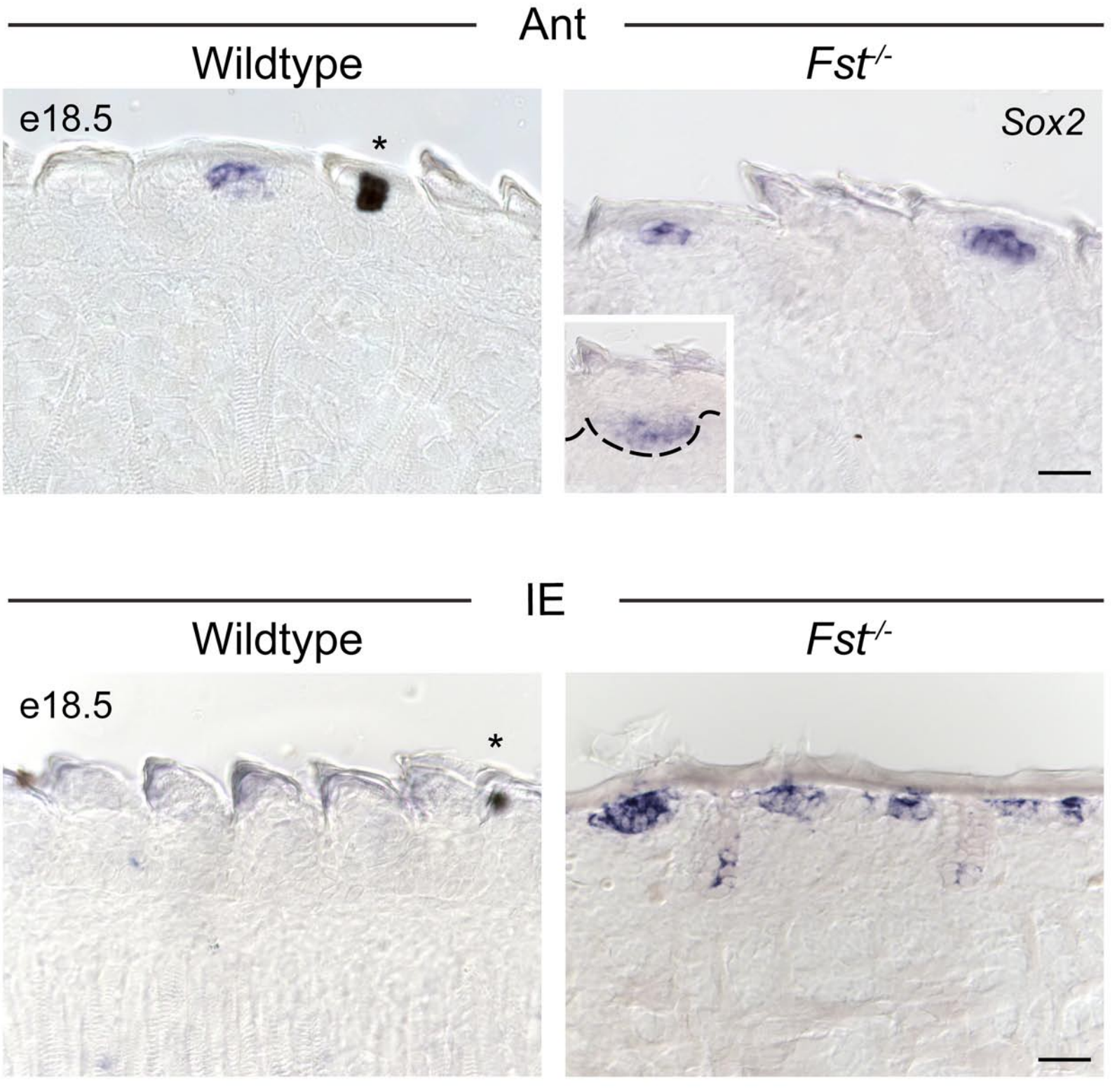
Ant
Wildtype
Fst-/-
e18.5
*
Sox2
IE
Wildtype
Fst-/-
e18.5
*

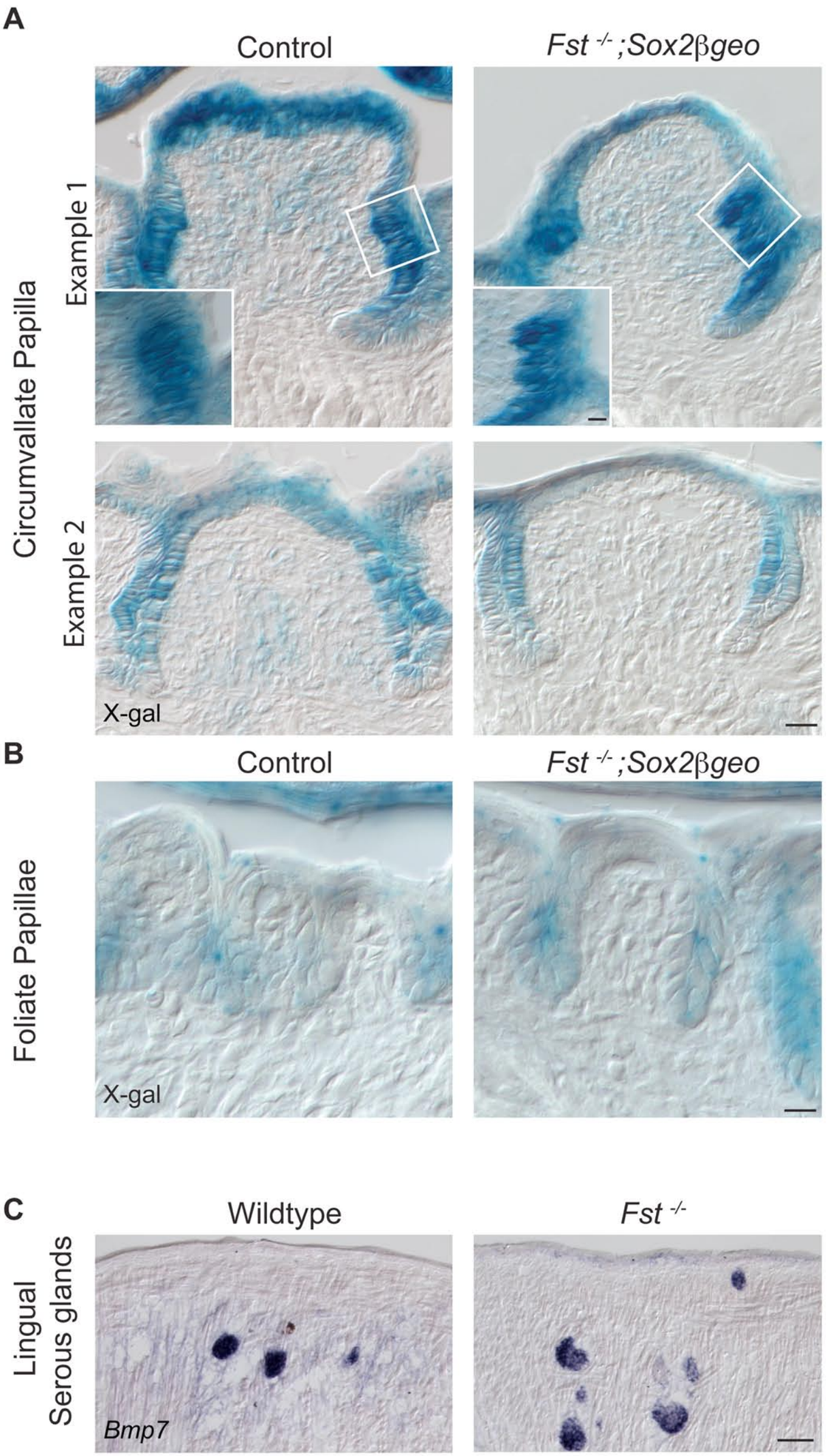
A
Control
Fst -/- ;Sox2βgeo
Circumvallate Papilla
Example 1
Example 2
X-gal
B
Control
Fst -/- ;Sox2βgeo
Foliate Papillae
X-gal
C
Wildtype
Fst -/-
Lingual Serous glands
Bmp7

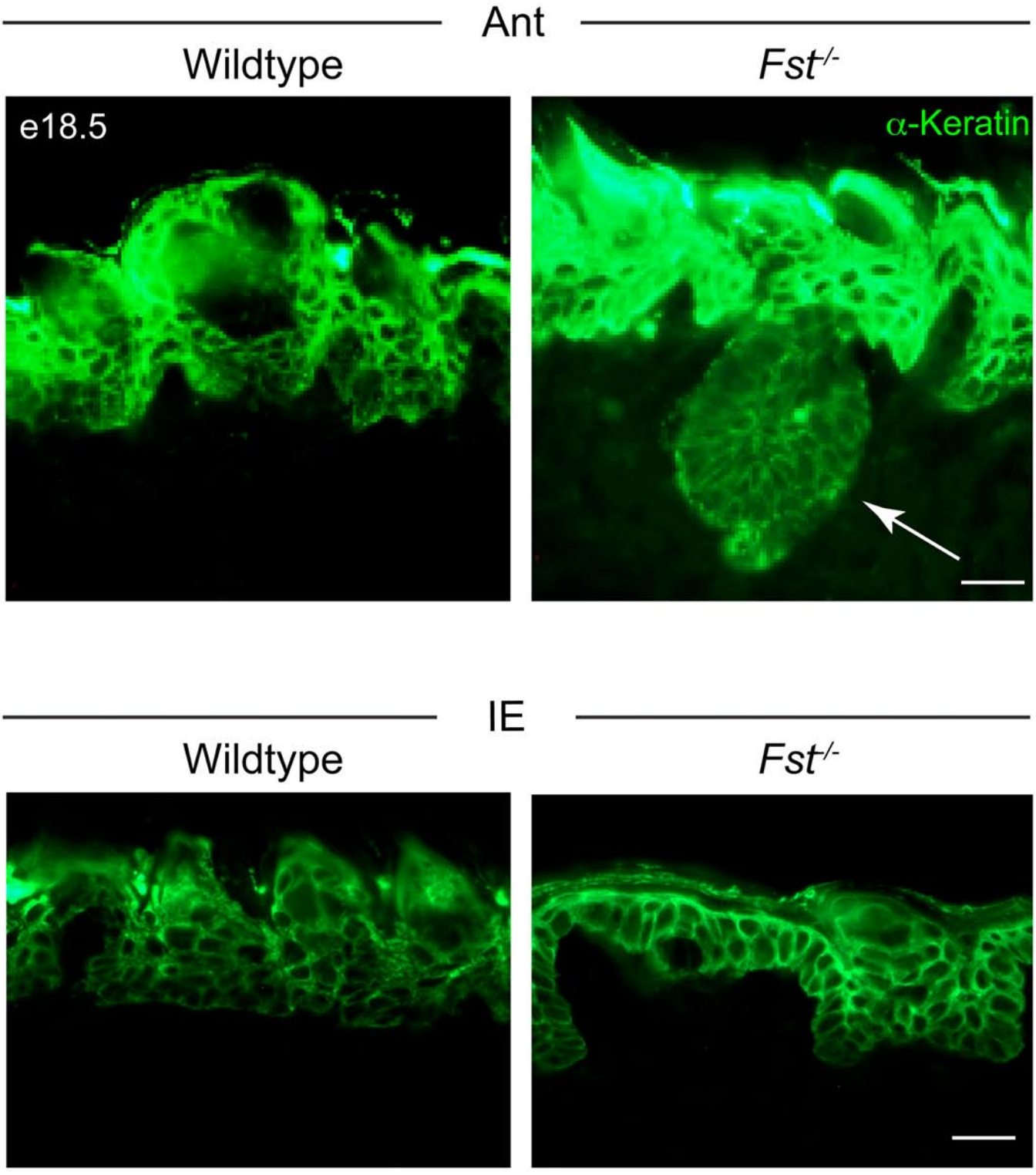
Ant
Wildtype
Fst-/-
e18.5
α-Keratin
IE
Wildtype
Fst-/-

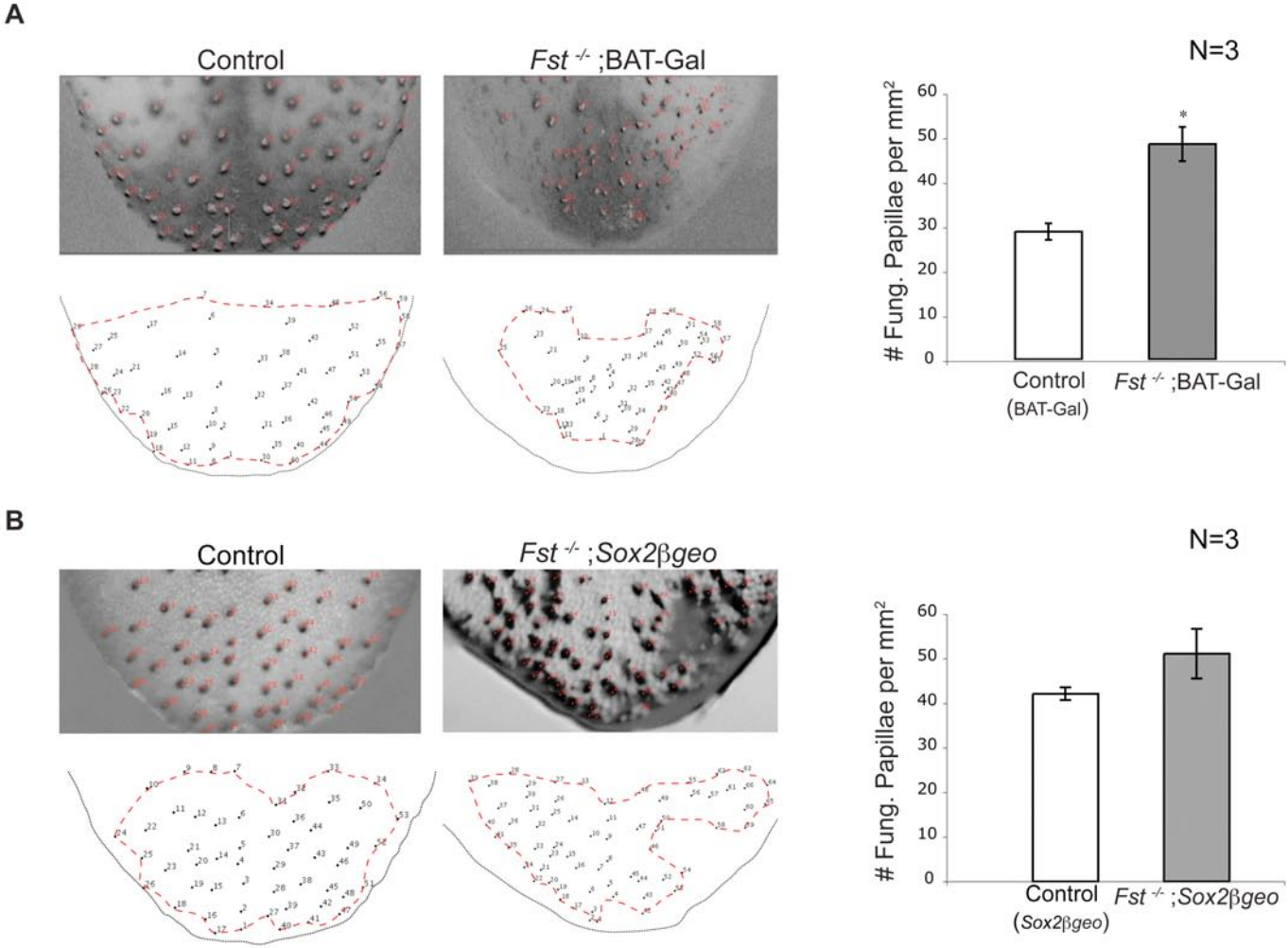
A
Control
Fst -/- ;BAT-Gal
N=3
# Fung. Papillae per mm2
60
50
40
30
20
10
0
*
Control
(BAT-Gal)
Fst -/- ;BAT-Gal
B
Control
Fst -/- ;Sox2βgeo
N=3
# Fung. Papillae per mm2
60
50
40
30
20
10
0
Control
(Sox2βgeo)
Fst -/- ;Sox2βgeo

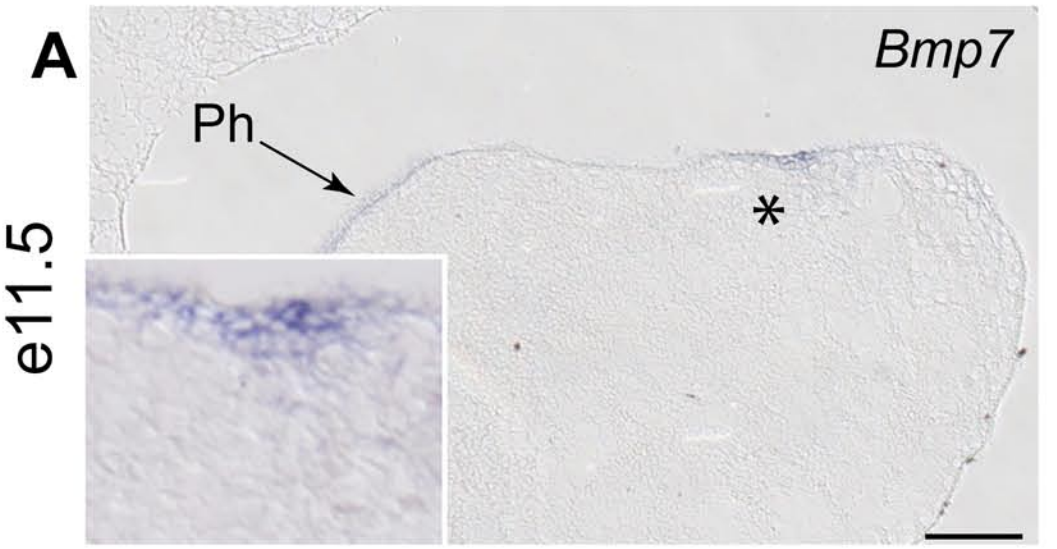
A
Bmp7
Ph
*
e11.5

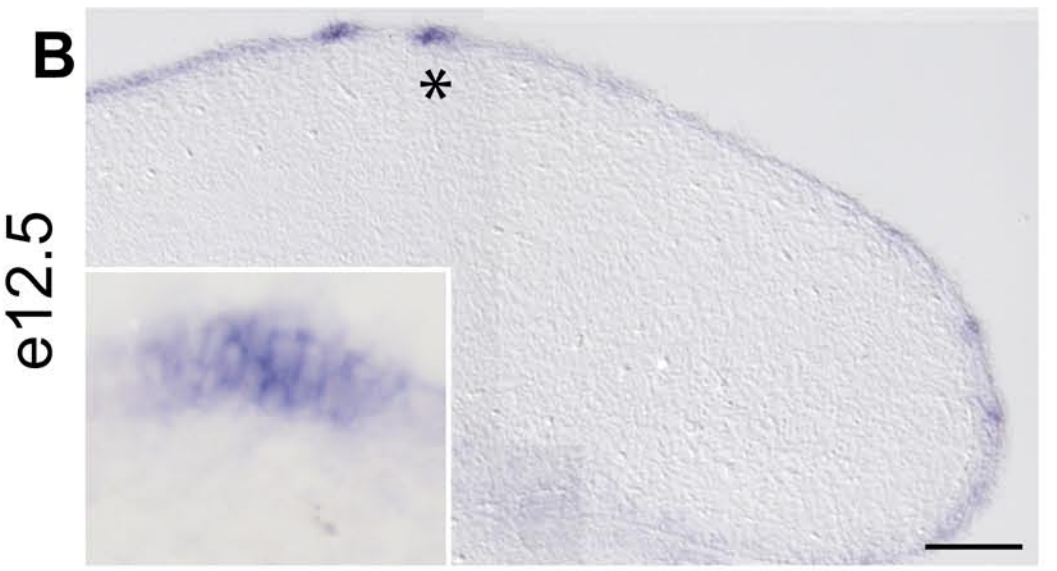
B
*
e12.5

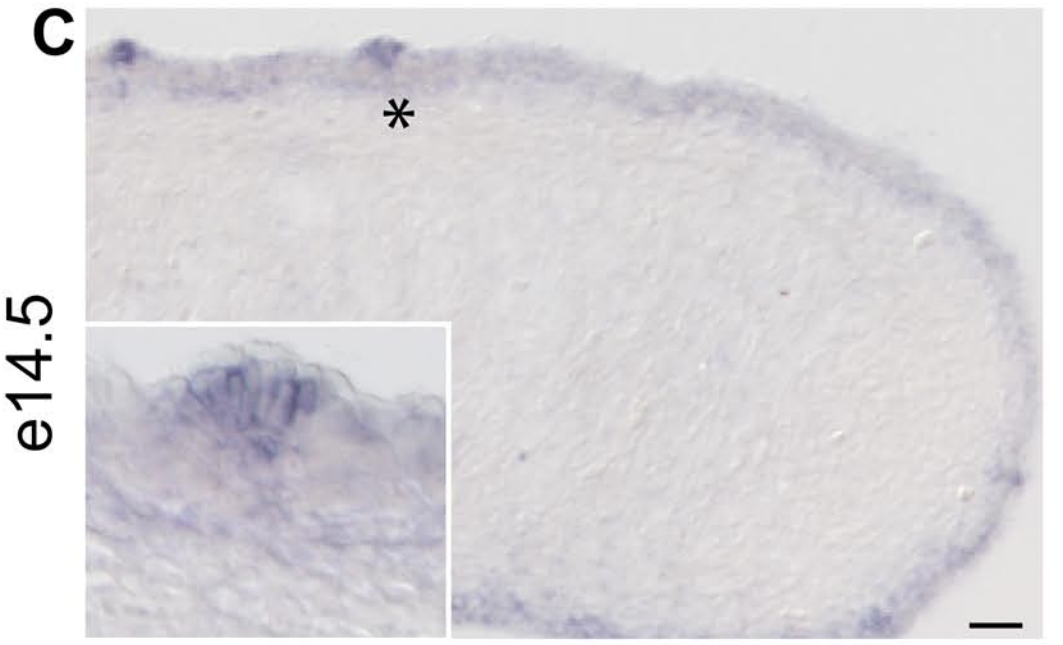
C
*
e14.5

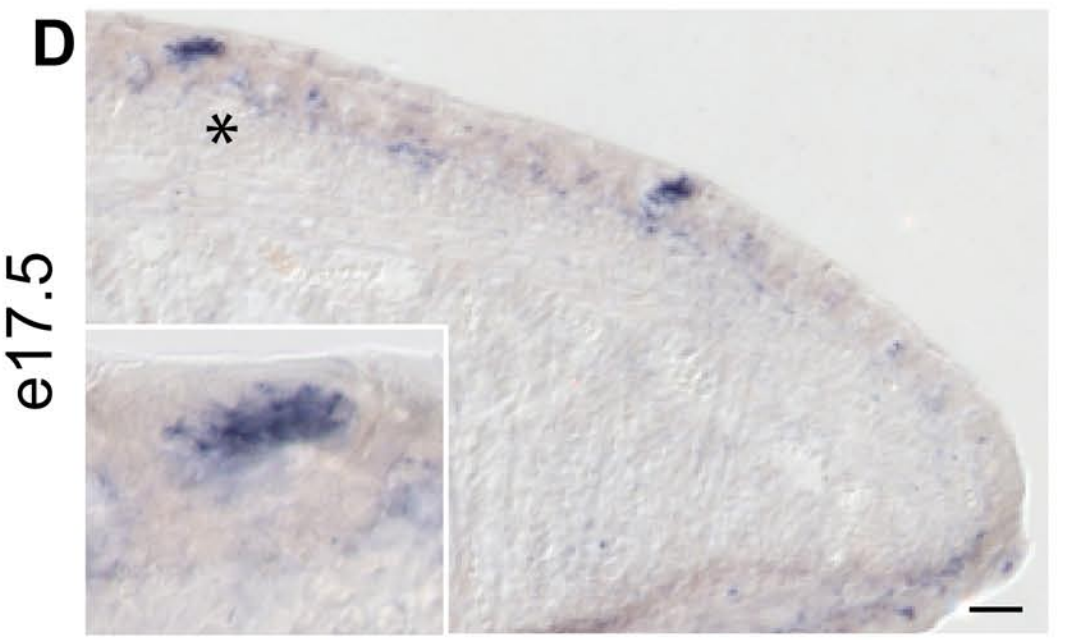
D
*
e17.5

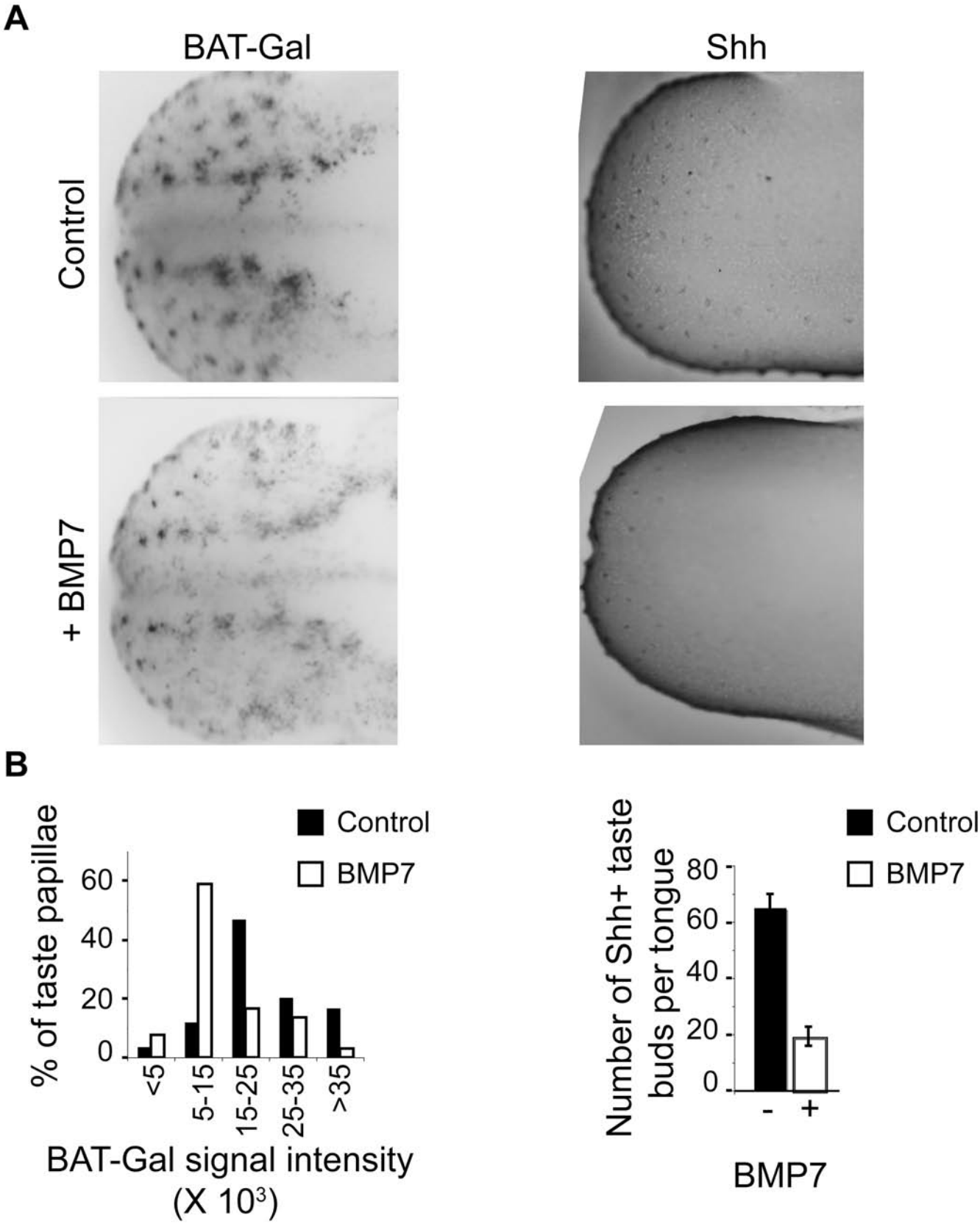
A
BAT-Gal
Shh
Control
+ BMP7
B
Control
BMP7
% of taste papillae
60
40
20
0
<5
5-15
15-25
25-35
>35
BAT-Gal signal intensity
(X 10³)
Number of Shh+ taste buds per tongue
80
60
40
20
0
-
+
BMP7

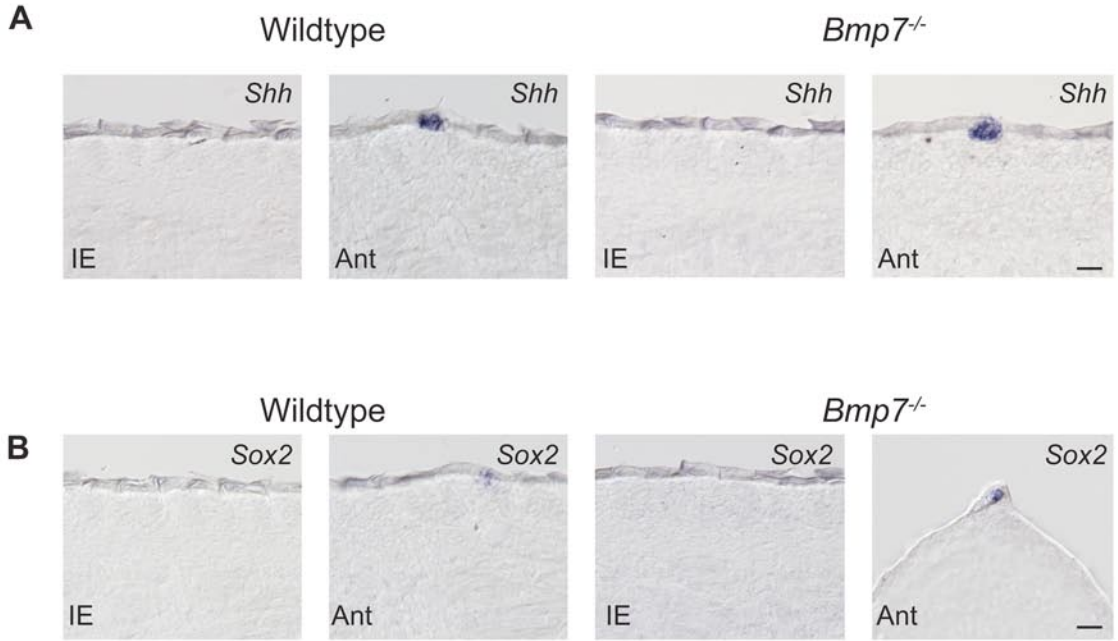
A
Wildtype
Bmp7-/-
Shh
IE
Ant
B
Sox2

- **This notebook makes use of the RDL package by Selwyn Hollis, which at the current time only runs on Mathematica 5. The results may still be viewed in higher versions of Mathematica**

  - **The following generates the "noise"**

```
<< Statistics`ContinuousDistributions`

list1 = Table[0.2 Random[LogNormalDistribution[0.3, 0.7]], {1000}];

<< Graphics`Graphics`

Histogram[list1]
```

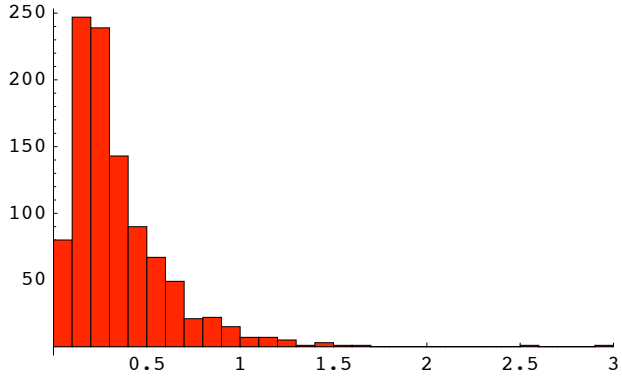

- Graphics -

```
h = 1 / 50; u0 = Table[0.2 Random[LogNormalDistribution[0.3, 0.7]], {y, 0, 1, h}, {x, 0, 3 / 2, h}];

ListDensityPlot[1.2 u0,  Mesh → False, ColorFunction → (GrayLevel[1 - #] &),
 PlotRange → {0, 2.5}, AspectRatio → 2 / 3, Frame → False]
```

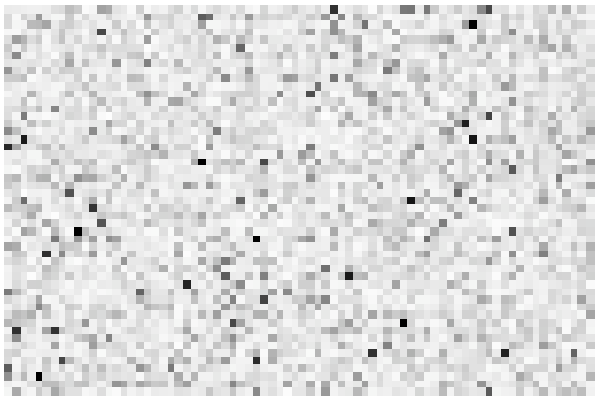

- DensityGraphics -

- **The following generates the pre-pattern**

```
u1 = Table[(Sin[15 x] Sin[15 y])^6, {y, 0, 1, h}, {x, 0, 3 / 2, h}];
ListDensityPlot[0.8 u1, Mesh → False, ColorFunction → (GrayLevel[1 - #] &),
 PlotRange → {0, 2.5}, AspectRatio → 2 / 3, Frame → False]
```

- DensityGraphics -

- **The following shows what the sum of the noise and prepattern looks like.**

```
u1 = Table[(Sin[15 x] Sin[15 y])^6, {y, 0, 1, h}, {x, 0, 3 / 2, h}];
ListDensityPlot[1.2 u0 + 0.8 u1, Mesh → False, ColorFunction → (GrayLevel[1 - #] &),
 PlotRange → {0, 2.5}, AspectRatio → 2 / 3, Frame → False]
```

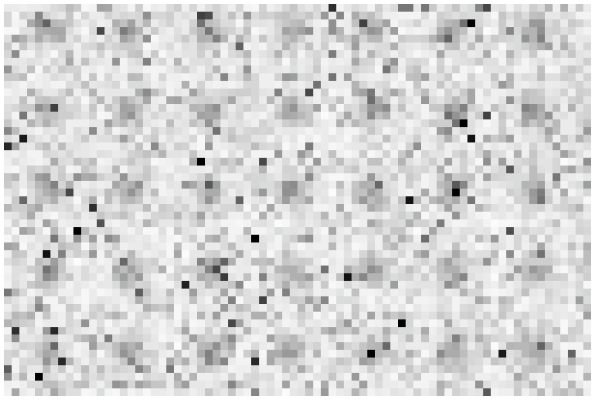

- DensityGraphics -

- **Next, RDL is loaded. This generates pairs of images for sequential time points. The image on the left is u (BMP7), and the one on the right is v (FST). Since FST is a constant, the image on the right may be ignored.**

```
<< RDL`ReactionDiffusionLab`

v0 = Table[1, {y, 0, 1, h}, {x, 0, 3 / 2, h}];

(*this makes FST=1 everywhere*)

SetOptions[RDDensityPlots, ColorFunction → (GrayLevel[1 - #] &)];
```

In the simulation below, FST is present and carrying out its normal function

```
actinhib := {11.43/v u^2/(u^2 + 2) - 3 u, 0};
d1 = .0005; d2 = .01; dt = .01 * h^2 / Max[{d1, d2}];
RDDensityPlots[actinhib, {u, v}, {1.2 u0 + 0.8 u1, v0}, {d1, d2}, dt, 30,
 PlotRange → {{0, 2.5}, {0, Automatic}}, PlotEvery → 100, ImageSize → 500, ReturnLast → True];
(*below are shown just the first, tenth, and twenty-fifth images*)
```

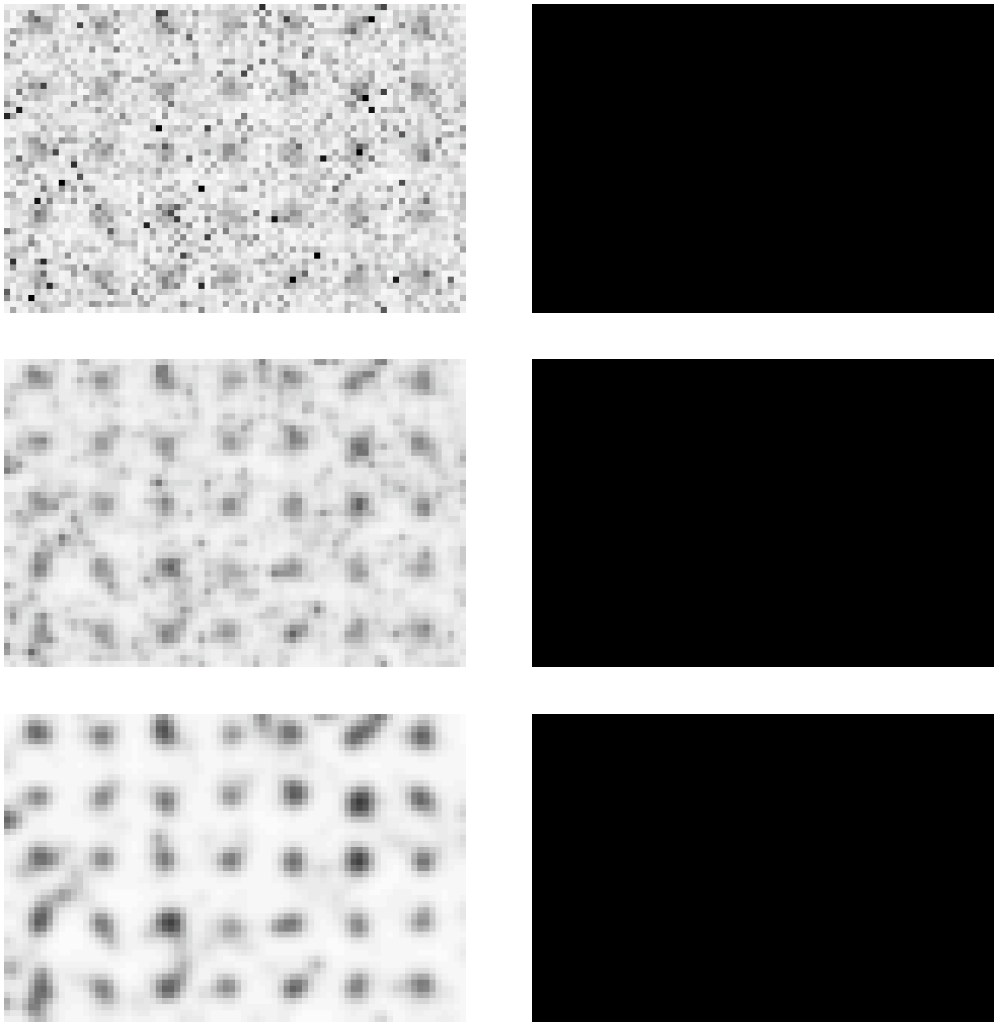

```
Max[Flatten[%]] (*this shows the highest value within the domain*)
```

```
2.17148
```

- **In the simulation below, the loss of FST was simulated by increasing the coefficient in front of the first term from 11.43 to 14.29**

```
actinhib := {14.29/v u^2/(u^2 + 2) - 3 u, 0};
d1 = .0005; d2 = .01; dt = .01 * h^2 / Max[{d1, d2}];
RDDensityPlots[actinhib, {u, v}, {1.2 u0 + 0.8 u1, v0}, {d1, d2}, dt, 30,
 PlotRange → {{0, 2.5}, {0, Automatic}}, PlotEvery → 100, ImageSize → 500, ReturnLast → True];
(*below are shown just the first, tenth, and twenty-fifth images*)
```

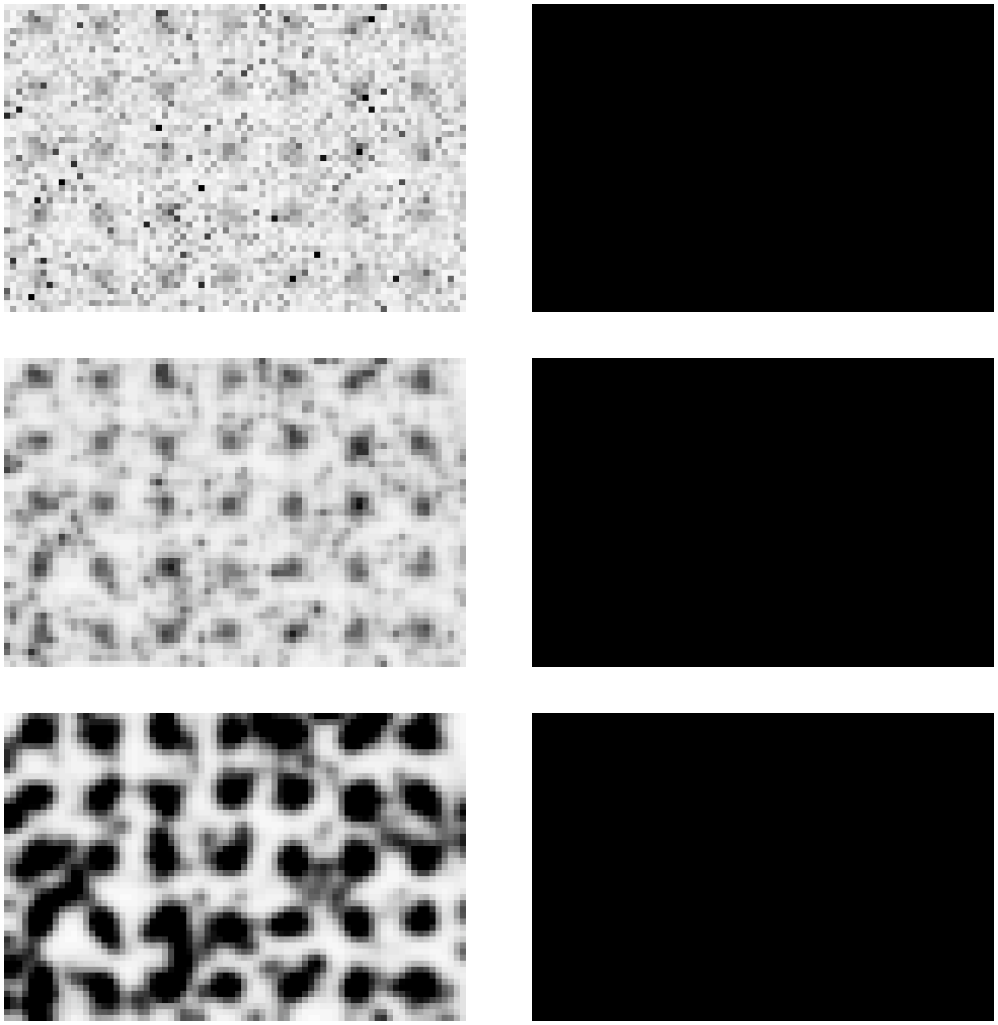

```
Max[Flatten[%]]
```

```
3.64044
```

- **A word about units and the plausibility of these parameter choices: If the unit of distance is cm, then the box shown here is 1x1.5 centimeters. Now let's say the unit of time is 50000 seconds. Then the diffusion coefficient that is used here of 5 x 10^{-4}, can be understood as representing $10^{-8}$when converted to units of seconds.**

Now when we plot every 100 time steps for 30 plots, that's 3000 time steps. If the time step duration is 0.0004, then the total elapsed time is 3000*0.0004 = 1.2 time units. And if the time unit=50000 seconds, then the total elapsed time is 60000 seconds = 1000 min = 16.7 hours.

Note, in the manuscript, the figures shown are from the 25th plot rather than the 30th. So that means they represent a time of 50000 seconds, or 13.9 hours.

These distances, times and diffusion coefficients are all within reasonable ranges for tongue development.

Table S1. Summary of phenotypes observed in tongues of *Fst*$^{-/-}$ versus wild-type mice

Anterior tongue (fungiform/filiform papillae)		Posterior tongue (intermolar eminence)	
Wild type	*Fst*$^{-/-}$	Wild type	*Fst*$^{-/-}$
Filiform papillae develop normally	Filiform papillae develop normally	Filiform papillae develop normally	No filiform papillae develop
Clear demarcation of epithelial-mesenchymal border	Dysplastic epithelial-mesenchymal border	Clear demarcation of epithelial-mesenchymal border	Dysplastic epithelial-mesenchymal border
Sox2 expressed in developing taste placode/taste bud	Excess and ectopic *Sox2*-positive domains	*Sox2* not expressed	Ectopic *Sox2*-expressing domains
Distinct patterning of papillae on anterior 2/3 of the tongue	Abnormal size and disrupted spacing of fungiform papillae	Filiform papillae only	Ectopic fungiform papillae-like structures
Wnt activity in developing taste placode/taste bud	Decreased Wnt activity	Wnt activity in filiform papillae only	Wnt activity in ectopic fungiform papillae-like structures
Shh expressed in developing taste placode/taste bud	Decreased *Shh* expression	*Shh* is not expressed	*Shh* expression in ectopic fungiform papillae-like structures
Fungiform papillae are innervated by projecting nerve fibers stained by PGP9.5	Normally is innervated	No visible innervation by PGP9.5 staining	Ectopic fungiform papillae-like structures are innervated
Gustducin expressed in taste receptor cells of the taste bud at postnatal stages	Premature gustducin expression	Gustducin is not expressed	Gustducin expression in ectopic fungiform papillae-like structures
Bmp7 expressed in developing taste placode/taste bud	Expansion of *Bmp7* expression domains	*Bmp7* is not expressed	Ectopic expression of *Bmp7*
Proliferating cells are concentrated along the epithelial-mesenchymal border and in the taste bud	No change in cell proliferation	Proliferating cells are concentrated along the epithelial-mesenchymal border	No change in cell proliferation